



HAL
open science

The Spike-and-reset dynamics for non-linear integrate-and-fire neuron models

Jonathan Touboul, Romain Brette

► **To cite this version:**

Jonathan Touboul, Romain Brette. The Spike-and-reset dynamics for non-linear integrate-and-fire neuron models. [Research Report] RR-6531, 2008. inria-00276924v2

HAL Id: inria-00276924

<https://inria.hal.science/inria-00276924v2>

Submitted on 29 Aug 2008 (v2), last revised 11 Jun 2018 (v5)

HAL is a multi-disciplinary open access archive for the deposit and dissemination of scientific research documents, whether they are published or not. The documents may come from teaching and research institutions in France or abroad, or from public or private research centers.

L'archive ouverte pluridisciplinaire **HAL**, est destinée au dépôt et à la diffusion de documents scientifiques de niveau recherche, publiés ou non, émanant des établissements d'enseignement et de recherche français ou étrangers, des laboratoires publics ou privés.



INSTITUT NATIONAL DE RECHERCHE EN INFORMATIQUE ET EN AUTOMATIQUE

*Spiking dynamics of bidimensional
integrate-and-fire neurons*

Jonathan Touboul — Romain Brette

N° 6531

August 29, 2008

Thème BIO

*R*apport
de recherche



Spiking dynamics of bidimensional integrate-and-fire neurons

Jonathan Touboul ^{*}, Romain Brette

Thème BIO — Systèmes biologiques
Projet Odyssée [†]

Rapport de recherche n° 6531 — August 29, 2008 — 46 pages

Abstract:

The class of non-linear integrate and fire neuron models introduced in [19], containing such models as the Izhikevich and the Brette-Gerstner ones, are hybrid dynamical systems, defined both by a continuous dynamics, the subthreshold behavior, and a discrete dynamics, the spike and reset process. Interestingly enough, the reset induces in bidimensional models behaviors only observed in higher dimensional continuous systems (bursting, chaos, ...). The subthreshold behavior (continuous system) has been studied in previous papers. Here we study the discrete dynamics of spikes. To this purpose, we introduce and study a Poincaré map which characterizes the dynamics of the model. We find that the behavior of the model (regular spiking, bursting, spike frequency adaptation, bistability, ...) can be explained by the dynamical properties of that map (fixed point, cycles...). In particular, the system can exhibit a transition to chaos via period doubling, which was previously observed in Hodgkin-Huxley models and in Purkinje cells.

Key-words: No keywords

^{*} jonathan.touboul@sophia.inria.fr

[†] Odyssée is a joint project between ENPC - ENS Ulm - INRIA

Spiking dynamics of bidimensional integrate-and-fire neurons

Résumé : The class of non-linear integrate and fire neuron models introduced in [19], containing such models as the Izhikevich and the Brette-Gerstner ones, are hybrid dynamical systems, defined both by a continuous dynamics, the subthreshold behavior, and a discrete dynamics, the spike and reset process. Interestingly enough, the reset induces in bidimensional models behaviors only observed in higher dimensional continuous systems (bursting, chaos, ...). The subthreshold behavior (continuous system) has been studied in previous papers. Here we study the discrete dynamics of spikes. To this purpose, we introduce and study a Poincaré map which characterizes the dynamics of the model. We find that the behavior of the model (regular spiking, bursting, spike frequency adaptation, bistability, ...) can be explained by the dynamical properties of that map (fixed point, cycles...). In particular, the system can exhibit a transition to chaos via period doubling, which was previously observed in Hodgkin-Huxley models and in Purkinje cells.

Mots-clés : Pas de motclef

In [19], the author introduces a class of nonlinear bidimensional integrate-and-fire neurons that is very interesting for the neuro-computing community. Indeed, they combine the computational simplicity of classical leaky integrate-and-fire neuron with the ability to reproduce a large number of behaviors recorded in intracellular experiments. These models also get rid of the dependency on a given threshold because of their property to diverge at the times of the spikes. These models are bidimensional nonlinear dynamical systems. One of the variables involved is interpreted as the membrane potential. The second variable models the adaptation of the nerve cell.

These models are spiking models: they are defined by a subthreshold dynamics governed by a continuous dynamical system, an nonlinear bidimensional ordinary differential equation. The dynamics of the adaptation variable is linear, and the dynamics of the membrane potential involves a nonlinear convex function F modeling the dynamics of ion channels. For instance in the Adaptive Exponential model [1], the sodium current responsible for the generation of action potentials is modelled by an exponential function, following the work of [7]. In this subthreshold dynamics, the nonlinearity plays an essential role. It governs many behaviors, as studied further in the paper [20]. Beyond this continuous dynamics is mapped a discrete dynamics defined by the spiking process. Indeed, after a spike emission, i.e. a divergence of the membrane potential, many solutions are possible. The reset condition at the times of the spike amounts resetting instantaneously the membrane potential to a given value, while the adaptation variable, which do not diverge at the time of the spikes, is added a fixed deterministic value corresponding to the spike-triggered adaptation.

Therefore, we will call these models hybrid dynamical systems, since they are defined by both a continuous and a discrete dynamical system. This structure make these models very interesting. Indeed, As observed in the different publications dealing with this type of models [9, 1, 19], the addition of the reset to the bidimensional continuous dynamical systems generates behaviors which cannot appear in autonomous bidimensional nonlinear ODEs, such as the bursting phenomenon and the existence of chaos. So far the different spiking patterns have only been simulated. Recently, Richard Naud studied together with Wulfram Gerstner and other colleagues [17] from a numerical point of view the emergence of the different spike patterns in one of the models of this class: the adaptive exponential model. In this paper we will rigorously study from a mathematical point of view these different behaviors, in order to understand qualitatively the origin of the different observed behaviors, and quantitatively to get insights on the ranges of parameters to obtain a given behavior.

In the first section, we deal with the mathematical framework we study in the whole paper. We introduce in this section an essential element to study the spike patterns observed: the adaptation (or Poincaré) map, and study some of its properties. We observe that the properties of this map are closely linked with the subthreshold dynamics properties, more precisely with the number and stability of fixed points, and with the possible presence of cycles. This is why we chose to organize the paper depending on the number and the type of fixed points of the subthreshold dynamics. The precise study of the properties of this map leads us to characterize qualitatively the different phasic and tonic behaviors. In

the case where the subthreshold system has no fixed point, we will provide general and simple conditions on Φ to get regular spiking and to distinguish between spike frequency adaptation and mixed mode, explain map the origin of bursting activity. When fixed points exists, the topological properties of the subthreshold dynamics and the structure of the attraction basins (stable fixed point) or stable manifold (saddle fixed point) will be very important to distinguish between phasic and tonic behaviors. In these cases, the map Φ can be discontinuous and therefore its properties are more intricate. The different behaviors observed qualitatively in each case lead us to study more precisely the bifurcations between these types of behaviors with respect to the subthreshold dynamics parameters. We will show that the model was able to present chaotic spiking trajectories, similar to those observed in detailed models such as the Hodgkin-Huxley model taking into account the temperature and that had also been observed in intracellular recordings of the Prukinje cell. Furthermore, the qualitative differences observed with respect to the subthreshold dynamics parameters leads us to study the bifurcations with respect to the subthreshold parameters also. This study will lead us to introduce electrophysiological classes, i.e. sets of parameters for which the neuron has qualitatively the same type of response depending on the stimulus intensity.

These results are the first rigorous study of the spiking mechanism for this kind of spiking model.

1 Basic definitions

1.1 The class of nonlinear models

The class of systems we study here is the one we introduced [19] to study its subthreshold properties. We recall here briefly for the sake of completeness the main definitions. In this class of models, The neuron's membrane voltage is the superpositions of two mechanisms: a nonlinear subthreshold integration mechanism, driven by the equation:

$$\begin{cases} \frac{dv}{dt} = F(v) - w + I \\ \frac{dw}{dt} = a(bv - w) \end{cases} \quad (1.1)$$

where a, b and I are real parameters and F is a real function accounting for the nonlinear ionic currents, satisfying the three assumptions ??, ??, ??. In order to ensure that the neuron will elicit spikes, we add the following assumption:

Assumption (A1). *There exists $\varepsilon > 0$ such that F grows faster than $v^{1+\varepsilon}$ when $v \rightarrow \infty$*

This subthreshold dynamics is coupled with a spike-and-reset mechanism: if the membrane potential blows up at time t^* , we consider that a spike is emitted, and subsequently the membrane potential is instantaneously reset to a constant value v_r and the adaptation variable is increased by a constant value d :

$$\begin{cases} v(t^*) = v_r \\ w(t^*) = w(t^{*-}) + d \end{cases} \quad (1.2)$$

where v_r is the value of the reset of the membrane potential and $d > 0$ a real parameter accounting for the spike-triggered adaptation.

This system is an *hybrid dynamical system*: it is defined by both a continuous time dynamical system given by the equations (1.1) and a discrete dynamical system called the spike and reset mechanism, given by the equations (1.2), with five real parameters (a, b, I, v_r, d) . The parameters (a, b, I) govern the subthreshold dynamics, while the parameters v_r and d govern the spike and reset mechanism. The subthreshold bifurcation problem was first studied by Izhikevich in [11] in the case of the adaptive quadratic integrate and fire model, and extended to the generalized class of models of [19]. It appears that a is not a bifurcation parameter, and that the system undergoes a subcritical Bogdanov-Takens bifurcation. Moreover, under a simple condition on F and the other parameters, the model can undergo a Bautin bifurcation. This analysis accounts for the subthreshold behavior of the neuron and allows one to define *electrophysiological classes* of neurons depending on the parameters of the model, as we will do in [20] in the case of the adaptive exponential model.

Nevertheless, this former study does not explain the spiking behaviors of the neuron, which are governed by the spike and reset mechanism. These properties are closely linked with topological properties of the underlying dynamical system, and we are interested here in understanding these properties. In this section we deal with the existence and uniqueness of solutions for this type of problems, and recall some of the main properties of the subthreshold dynamical system.

1.2 Existence and uniqueness of solution

The Cauchy problem consists in proving whether there exists a unique solution to this problem defined on \mathbb{R}^2 given an initial condition. This problem was addressed by Romain Brette in [2] in the case of spiking models defined by a one dimensional ODE with a finite spiking threshold and a reset condition. He found that the reset introduced a countable and ordered set of backward solutions for a given initial condition. He shows that beyond the mathematical interest of this question, it had important implications in terms of neural coding, considering that the set of possible output spike trains in response to a given input corresponds to the set of solutions defined on \mathbb{R} .

In the present case we observe the same structure as in the case of one-dimensional models. First of all, we can readily prove that we have existence and uniqueness of solution for the forward equation.

Proposition 1.1. The equations (1.1) and (1.2), together with initial conditions (v_0, w_0) at time t_0 has a unique solution defined for $t \geq t_0$.

Proof. Because of the regularity condition ??, Cauchy-Lipschitz theorem of existence and uniqueness of solution applies until the solution blows up. If the solution keeps bounded, then we have existence and uniqueness of solution. If the solution blows up at time t^* , then we are reset to a unique point, defined by the reset condition 1.2, and we are again in the case we already treated starting from $(v_r, w(t^*) + d)$ at time t^* . We can apply this mechanism

again provided that the value of $w(t^*)$ is finite. This is true because of assumption (A1). Indeed, in that case, when $v \rightarrow \infty$, the equation of the trajectory in the phase plane reads:

$$\frac{dw}{dv} = \frac{a(bv - w)}{F(v) - w + I}$$

and this equation is integrable for $v \rightarrow \infty$. Furthermore, to be able to prove the existence and uniqueness of solution for all $t \geq t_0$, we need to ensure that the spike time does not tend to 0 (i.e. spikes do not accumulate at a given time location). The spike time decreases when the reset location on the w axis decreases also. When w_0 is small enough, the value of the adaptation variable is increasing all along the trajectory and therefore the new reset location will be greater than the former one, and hence it is impossible that this reset value tends to $-\infty$ (the precise study of the trajectories that will be lead in the sequel we provide a further insight of this property). Therefore, the spike times have a lower bound on this trajectory, and between two spike times, we can prove a property of existence and uniqueness of solution. Therefore we have existence and uniqueness of a solution starting from (v_0, w_0) which is defined for any $t \geq t_0$. \square

In this proposition, we proved that there existed a unique forward solution to the problem for a given initial condition. The backward problem is slightly more complex, and can be treated in the same fashion as done in [2]. Let (v_0, w_0) be a given initial condition at t_0 . In the case of a finite threshold, to have existence of a backward solution one had to ensure that the backward solution will not cross the threshold. In our case this is not possible because of the structure of the equations (the membrane potential cannot tend to infinity in finite time for the backward problem). But a new issue appears: the membrane potential can tend to $-\infty$ in finite time. In this case no admissible backward solution exists. If the non-spiking backward solution tends to $-\infty$ in finite time and furthermore if this trajectory does not cross the line $v = v_r$, then there is no backward solution admissible. We will study further this issue below, because we need more information on the reset dynamics.

1.3 Subthreshold bifurcations

Because of existence and uniqueness of solution obtained in proposition 1.1, we conclude that the whole dynamics between two spikes depends only on the initial condition of the neuron. The way the elicits a spike is mainly linked with the subthreshold dynamics, and define electrophysiological classes depending on the subthreshold dynamics parameters a , b and the input current I . This issue has been investigated in [19, 20]. We summarize here the results obtained. Let us denote $v^*(x)$ the unique solution, when it exists, of the equation $F'(v^*(x)) = x$. Let us denote by $F'_{-\infty}$ the limit of $F'(x)$ for $x \rightarrow -\infty$. This value can be either finite (but nonpositive) or equal to $-\infty$. Note that because of the strict convexity assumption, if there exists a solution, it is unique. Furthermore, solutions exist for any $x \in (F'_{-\infty}, \infty)$. Let us denote also $m(x) = F(v^*(x)) - xv^*(x)$. It is the unique minimum, when $v^*(x)$ exists, of $t \mapsto F(t) - xt$. We have:

Theorem 1.2. *The number and the stability of the fixed point of the subthreshold system depends on the parameters of the system in the following fashion:*

1. If $I > -m(b)$, then the system has no fixed point.
2. If $I = -m(b)$, then the system has a unique fixed point, $(v^*(b), w^*(b))$, which is non-hyperbolic. It is unstable if $b > a$. Along this curve in the parameter space (I, b) , the system undergoes a saddle-node bifurcation provided that $F''(v^*(b)) \neq 0$.
3. If $I < -m(b)$, then the dynamical system has two fixed points $(v_-(I, b), v_+(I, b))$ such that

$$v_-(I, b) < v^*(b) < v_+(I, b).$$

The fixed point $v_+(I, b)$ is a saddle fixed point, and the stability of the fixed point $v_-(I, b)$ depends on I and on the sign of $(b - a)$:

- (a) If $b < a$, the fixed point $v_-(I, b)$ is attractive.
- (b) If $b > a$, it depends on the input current I with respect to the value $I^*(a, b) = bv^*(a) - F(v^*(a))$.
- (c) At the point $b = a$ and $I = -m(a)$, the system undergoes a Bogdanov-Takens bifurcation provided that $F''(v_a) \neq 0$. Therefore, from this point, there is a saddle homoclinic bifurcation curve characterized in the neighborhood of the Bogdanov-Takens point by

$$(P) := \left\{ (I, b \geq a) ; I_{SHom} = -m(a) + \frac{12}{25} \frac{(b-a)^2}{F''(v^*(a))} + o(|(b-a)^2|) \right\}. \quad (1.3)$$

- i. If $I < I^*(a, b)$, the fixed point $v_-(I, b)$ is attractive.
- ii. If $I > I^*(a, b)$, the fixed point $v_-(I, b)$ is repulsive.
- iii. On the parameter line given by

$$(AH) := \left\{ (b, I) ; b > a \text{ and } I = bv^*(a) - F(v^*(a)) \right\},$$

the system undergoes an Andonov Hopf bifurcation, whose type is given by the sign of the variable

$$A(a, b) = F'''(v^*(a)) + \frac{1}{b-a} F''(v^*(a))^2.$$

If $A(a, b) > 0$, then the bifurcation is subcritical, and if $A(a, b) < 0$, then the bifurcation is supercritical. If furthermore we have $F'''(v^*(a)) < 0$ and some technical conditions fulfilled, then the system undergoes a Bautin bifurcation at the point $v^*(a)$ for $b = a - \frac{F''(v^*(a))^2}{F'''(v^*(a))}$ and $I = bv^*(a) - F(v^*(a))$.

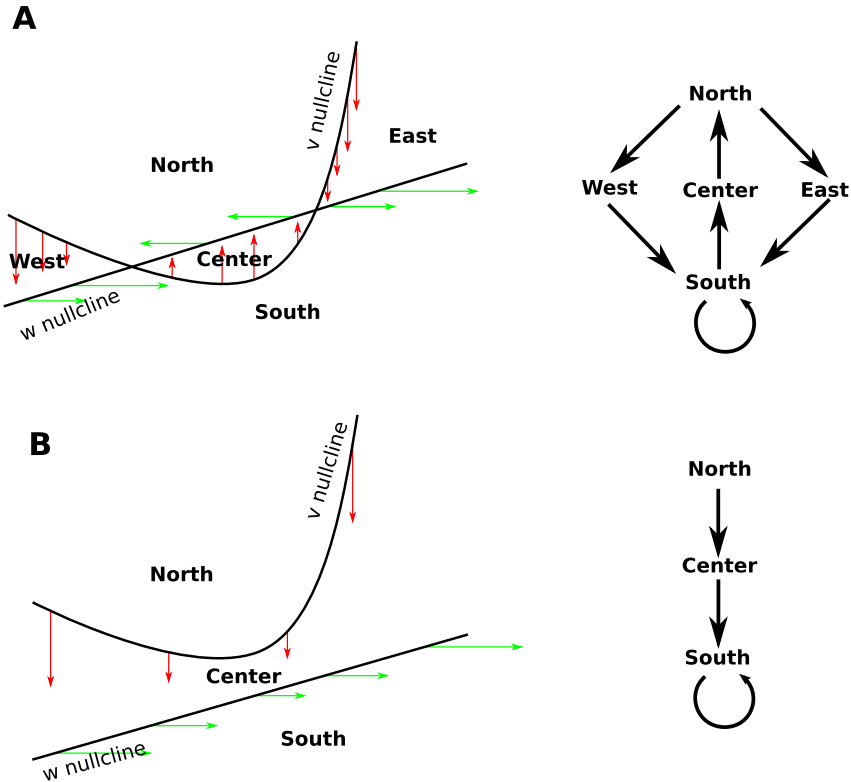


Figure 1: Nullclines of the dynamical system (horizontal axis: v ; vertical axis: w). A. The nullclines intersect in two points, and divide the phase space into 5 regions. The potential V increases below the V -nullcline, w increases below the w -nullcline. The direction of the flow along each boundary gives the possible transitions between regions (right). Spiking can only occur in the South region. B. The nullclines do not intersect. All trajectories must enter the South region and spike.

To describe further the subthreshold dynamics we consider that the phase plane is either separated in three or five regions, depending on the existence of fixed points or not. The description of these regions and the dynamics of the system between these regions is given in figure Fig.1. Note that in the case of 1.A, a trajectory in the South region can either keep in the south region or quit this region to enter the center region. Similarly, in the North region, it can either go East or West. We will precise this diagram later on in section 1.4.

The results on local and global bifurcation given in theorem 1.2 imply the existence of families of cycles, which we study further in the next section.

1.3.1 Periodic orbits

In this section we deal with the problem of characterizing the number and the type of limit cycles of the system. The problem of determining the number and location of limit cycles for an autonomous planar vector field is a very complex problem for general dynamical systems, and the case of a polynomial vector fields is still unresolved¹. Nevertheless, for simple systems such as the one we are studying here,

First of all, in the case $I > -m(b)$ (i.e. no fixed point for the subthreshold dynamics), it is clear that no limit cycle can exist, because of the shape of the vector field (see figure 1A.). Indeed, all the trajectories in the South region are trapped in this region, where the membrane potential v is strictly increasing, and therefore no cycle can appear.

When decreasing the current, the system will undergo a saddle-node bifurcation, two fixed points will appear, but no cycle will be generated. Hence the system has no cycle for $b < a$.

For $b > a$, when decreasing further the input current, the system will undergo a Hopf bifurcation, which will generate a branch of limit cycles. These limit cycles are repulsive if the system does not undergo a Bautin bifurcation, and are attractive if the system does and $b > a - \frac{F''(v^*(a))^2}{F'''(v^*(a))}$. The saddle-node and Andronov-Hopf bifurcations collide via a Bogdanov-Takens bifurcation at the point $b = a$. In the neighborhood of this bifurcation, the family of limit cycles collide with the saddle fixed-point manifold and disappears via a saddle-homoclinic bifurcation. The curve of saddle homoclinic bifurcations has the expansion near $b = a$ given by equation (1.3), and can be completely computed numerically using a continuation algorithm. In the neighborhood of the Bogdanov-Takens bifurcation, this curve exists and it can be continued on a semi-open interval in the parameter b , which we denote $[b, sh)$ where sh can be either infinite, or finite if the value of the current of the homoclinic bifurcation tends to $-\infty$.

There is no other bifurcation in the system, hence no other cycle can appear spontaneously.

Because of the structure of our vector field presented in figure 1.B., the cycles necessarily include the fixed point v_- , and do not include the fixed point v_+ , because the South zone intersected with the set $\{v \geq v_+\}$ is stable and no trajectory can escape from this zone.

¹it is the 16th of the 23 problems of David Hilbert

These cycles appear around the fixed point v_- , and then inflates until reaching the saddle fixed point v_+ .

In this paper, the structure of the attraction basin of the stable fixed point when it exists, of the stable limit cycle when it exists, and of the stable manifold of the saddle fixed point will play an important role. We describe their structure and topology in the next section.

1.4 Stable manifold and attraction basins

In planar dynamical systems, there exist two types of bounded trajectories stable trajectories: fixed points and periodic orbits. The dynamical systems analysis we did in [19] lead us to identify all the possible fixed point, and a family of periodic orbits, the one that is generated via Hopf bifurcation. In general, the problem of finding periodic orbits in a dynamical system is very hard to handle formally. In this section we deal with these problem in the particular case of the nonlinear neuron model we consider.

We are interested in this section in the structure of the attraction basins of bounded trajectories. A point (v, w) belongs to the attraction basin of a stable trajectory if and only if the system (1.1) starting from this point converges towards this trajectory. The topology of this set is governed by the subthreshold dynamics, and the problem of identifying in a closed form the attraction basin of the bounded solutions is very hard to handle formally. Nevertheless in our case, when such a bounded stable trajectory exists, there always exists a saddle fixed point. We will see that the structure of the attraction basin will be closely related to the structure of the stable manifold of the saddle fixed point, which helps us describing qualitatively these basins of attraction.

We now describe in detail the structure of the attraction basins of the stable fixed point or of the stable limit cycle when they exist, and the shape of the stable manifold of the saddle-fixed point when it exists (i.e. when $I < -m(b)$).

First of all, in the case where $b > a$ and $I \in (I_{SHom}, I_{Hopf})$, there exists a periodic orbit circling anti-clockwise around the stable fixed point. First of all, since this orbit is a trajectory of the dynamical system, no solution can cross it because of Cauchy-Lipschitz theorem. The attraction basin of the stable fixed point will therefore be delineated by the periodic orbit: any trajectory starting inside this zone delineated by the periodic orbit will necessarily converge to the fixed point because of Poincaré-Bendixon's theorem, and no solution starting outside this zone can converge towards this fixed point because trajectories will not cross (Cauchy-Lipschitz' theorem). The structure of the stable manifold in that case is also influenced by the shape of this periodic orbit. As already stated, the saddle fixed point is outside that cycle. For $v \geq v_+$, the stable manifold will be inside the v -nullcline, because of the direction of the eigenvectors of the Jacobian matrix at this point, and therefore this part of the manifold will stay in the north zone and this curve will be an increasing function of v . For $v < v_+$, the stable manifold winds around this cycle in the south, center, north and west zone. Indeed, the stable manifold is a trajectory of the phase plane converging to the saddle fixed point. This manifold is therefore a solution of the backward equation. For the backward equation, two cases can appear: either the solution tends to minus infinity, or it is a bounded trajectory. If it is a bounded trajectory, because of Poincaré-Bendixon's theorem,

it will either converge to a fixed point or to a periodic orbit. There is no stable fixed point reachable by the unstable manifold (the stable fixed point is repulsive for the backwards dynamics). Necessarily, this trajectory will converge to the limit cycle. Indeed, if it was not the case, this stable manifold will separate two zones, one of which containing the unstable limit cycle and the stable fixed point. Any trajectory starting in the zone containing the stable fixed point will either converge to the fixed point if it is inside the attraction basin of this fixed point, which is delineated by the unstable periodic orbit, or will be trapped inside this zone and will not enter inside the periodic orbit. This the latter case, this trajectory will not diverge because of the structure of the trajectories. Poincaré-Bendixon theorem would imply that there exists a stable fixed point or a stable periodic orbit in this zone which is not the case. Therefore trajectory cannot be trapped, and the stable manifold will wind around the Hopf limit cycle (see figure 2(a)).

In the cases where there is no unstable limit cycle around the stable trajectory, i.e. for $b < a$, or $b > a$ and $I < I_{\text{cycle}}$ in the case of fixed points, or in the case where the stable trajectory considered is a periodic orbit, the attraction basin of the stable fixed point and the stable manifold will be quite different. In these cases indeed, the attraction basin will no more be a closed curve, and will be deduced from the shape of the stable manifold. From the position of the nullclines and the eigenvectors of the Jacobian matrix at the saddle fixed point, it appears that the stable manifold must cross the saddle fixed point from above both nullclines (North) to below both nullclines (South). It follows that the side above the nullclines is the graph of an increasing function of V , like in the previous case. For the other part of the manifold, several cases can occur:

- if the stable manifold of the saddle fixed point crosses both nullclines, for instance when $F'_{-\infty} > -\infty$ and if $b \geq \frac{(F'_{-\infty} + a)^2}{4a}$ (see ??), then the separatrix will have the shape presented in figure 2(b),
- if only the w-nullcline is crossed (which will always be the case when $a < -F'_{-\infty}$, and the separatrix will have the shape presented in figure 2(d),
- in the case where it crosses no nullcline, the separatrix is the graph of an increasing function of v and is unbounded, like represented in figure 2(c).

1.5 Heteroclinic orbits

In the case where there are two unstable fixed point, one of which is repulsive and the other saddle, then the stable manifold of the saddle fixed point will still be the graph of an increasing function of v for $v \geq v_+$, and in the submanifold starting from $v < v_+$ will connect to the repulsive fixed point, for the same reason as mentionned in the case of the presence of an unstable limit cycle. Indeed, if we consider the backward equation starting in the neighborhood of the saddle fixed point, the repulsive fixed point of the forward dynamics becomes attractive, and it is the unique bounded trajectory possible. The stable manifold when considering the backward equation will either converge to the fixed point, or will diverge, according to Poincaré-Bendixon's theorem. But assuming that it is unbounded

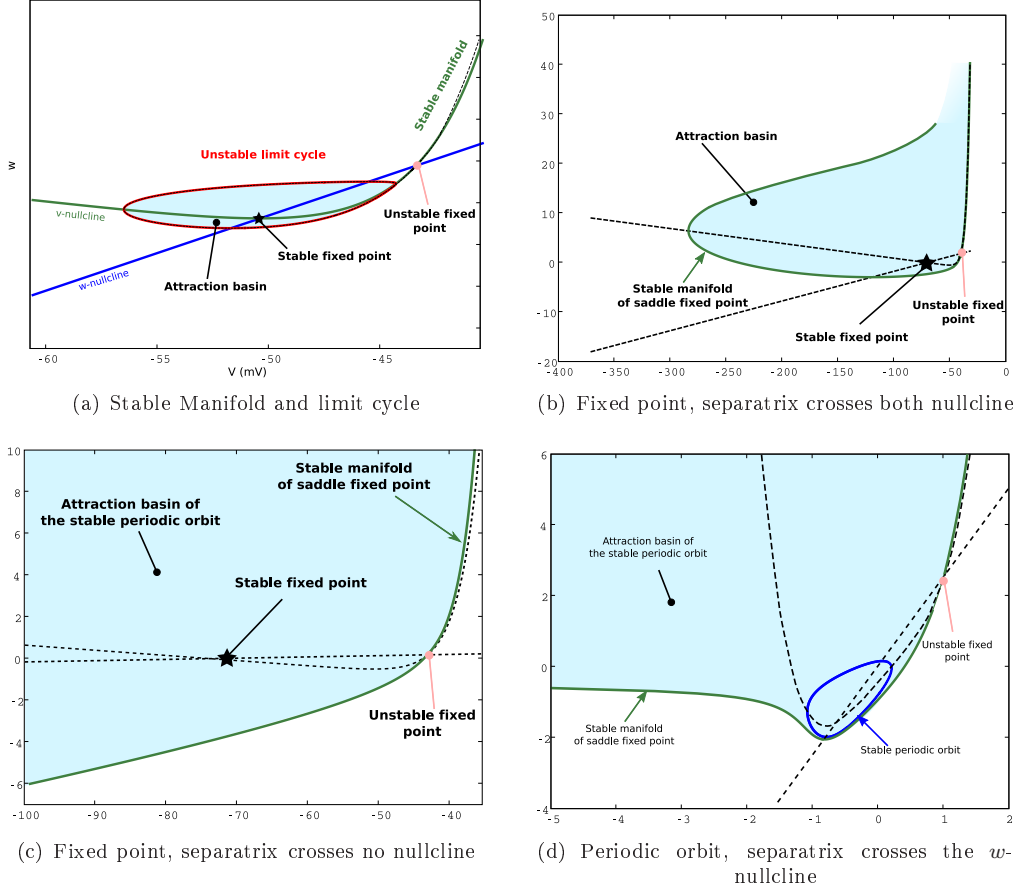


Figure 2: Representation of the attraction basin and the stable manifold of the saddle fixed point in different cases. Figure 2(a) corresponds to the case where there exists a repulsive limit cycle around the stable fixed point. The red line corresponds to this fixed point, the back dashed line to the stable manifold (see the indications in the figure). In the other three figures, we represented the case where there is no limit cycle in the phase plane. The dashed black line represent the nullclines, the green line the stable manifold of the saddle fixed point and the blue region the attraction basin of the stable trajectory. Figure 2(b) corresponds to the case where the separatrix crosses both nullclines: it returns in the direction $v > 0$ but will never reach the other part of the stable manifold (case of the AdExp model with original parameters but $a = 2g_L$ and $\tau_m = \tau_w$); 2(c) is the case where the stable manifold crosses no nullcline: it is the graph of an increasing function of v which delineates the attraction basin of the stable fixed point ((case of the dimensioned AdExp model with the original parameters but $a = 2g_L$ and $\tau_w = \tau_m/3$); 2(d) is the case where the stable manifold only crosses the w -nullcline. It was represented in the case where the stable trajectory is a periodic orbit (quartic model, $a = 1$, $b = 2.51$, $I = -0.5$).

leads to a contradiction: if it is unbounded, it separates two zones (see figure 2), one of which

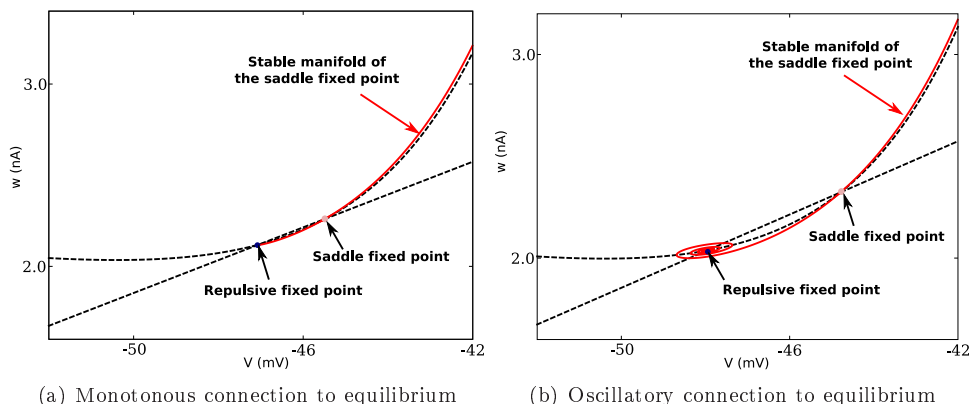


Figure 3: Stable manifold of the saddle fixed point in the case of two unstable equilibria. Dashed black curves are the nullclines of the system and the red curve is the stable manifold.

containing the unstable fixed point. A trajectory having its initial condition in this zone will be trapped in it for all $t > 0$. But in this zone, the trajectory will be bounded because of the structure of the vector field, but there is no fixed point nor stable periodic orbit. Therefore Poincaré-Bendixon's theorem leads to a contradiction, and the stable manifold necessarily connects to the repulsive fixed point. This connection can be one of two types (see figure 3: a monotonous connection in the case where the eigenvalues of the Jacobian matrix of the repulsive fixed point are real, and an oscillating connection when the eigenvalues have a non-nul imaginary part. This branch of stable manifold is therefore an heteroclinic orbit, connecting a repulsive equilibrium to a saddle equilibrium. It is structurally stable, and disappears at the Hopf bifurcation. In the case where the Hopf bifurcation is subcritical, the heteroclinic orbit connecting the repulsive fixed point and the saddle fixed point converts into an heteroclinic orbit connecting the saddle fixed point with the repulsive limit cycle. In the case where the Hopf bifurcation is supercritical (after Bautin bifurcation) the heteroclinic orbit will simply disappear.

1.6 Symbolic dynamics and spiking regions

This further study lead us to make the diagram 1 more precise, and get a symbolic dynamic for the subthreshold system. When there is no fixed point in the subthreshold system, the diagram given in 1.B. gives a symbolic dynamics for the evolution of the system, but it was not the case for diagram 1.A. in the South and the North regions. The knowledge of the stable manifold helps us to give a better understanding of the regional dynamics of the system. When fixed points exist, we characterized the stable manifold of the saddle fixed

point. It is composed of two submanifold, one of which is fully included in the North zone, which we denote Γ^+ , and the other one Γ^- which can be either an heteroclinic orbit, that can wind around the possible unstable limit cycle, or that can be unbounded. This curve Γ^- starts in the South region of 1.A. and then either connects to the repulsive fixed point (case of a “monotonous” heteroclinic orbit of figure 3(a)), or keep under the w -nullcline and stay in the South region (case of figure 2(c)), or enters the West region.

We distinguish two cases. When a stable trajectory exists (fixed point or periodic orbit) in the system, the attraction basin of this zone constitutes a stable region under the dynamics, which we call the *rest* region. Otherwise, in all the cases, there exists another stable region under the dynamics, which we call the *bottom* region, and which is the zone delineated by the minimum between the w -nullcline and the curve Γ^- . The *right* region is delineated by the curve Γ^+ on the left, and down by the w -nullcline. Eventually, there exists possibly a *up* region. The right and the up region go in finite time in the bottom region where they are trapped. These regions form a Markov partition of the dynamics. Interestingly enough, with this symbolic coding, we can see that every initial condition that is not inside the rest zone will eventually be after a finite time in the bottom region. This is very important in terms of spikes. Indeed, we can prove that for any initial condition in the bottom region, the membrane potential v will blow up in finite time, and therefore a spike will be emitted. Indeed, let (v_0, w_0) be a given initial condition in the bottom region at time t_0 . According to the shape of the vector field, as presented in our Markov partition, the whole trajectory will be trapped in this zone. But in this zone, we always have $w \leq v$ and therefore for all $t \geq t_0$ we have $w(t) \leq v(t)$. According to Gronwall’s theorem, the membrane potential at time $t \geq t_S$ will be greater or equal to the solution of:

$$\begin{cases} \dot{\tilde{v}} &= F(\tilde{v}) - b\tilde{v} + I \\ \tilde{v}(t_S) &= v(t_S) \end{cases}$$

which blows up in finite time by the virtue of assumption (A1).

Therefore any trajectory entering the bottom region will spike, and furthermore any trajectory having its initial condition outside the rest region will fall in the bottom region in finite time, and therefore elicit a spike.

Therefore we have been able to determine the regions of initial conditions where the neuron spikes. But this description does not account for the spike patterns produced by a given neuron which heavily relies on the reset process. The main tool we will use to qualify the spikes dynamics will be the discrete map governing the evolution of the adaptation reset point, which we will call the Poincaré application or the adaptation map.

1.7 The Poincaré application

The main tool we will use to characterize the spike patterns will be a discrete map, the Poincaré (or adaptation map), defined as follows.

Definition 1.1 (The adaptation (Poincaré) map). We denote by \mathcal{D} the domain of adaptation values w_0 such that the solution of (1.1) with initial condition (v_r, w_0) blows up in finite

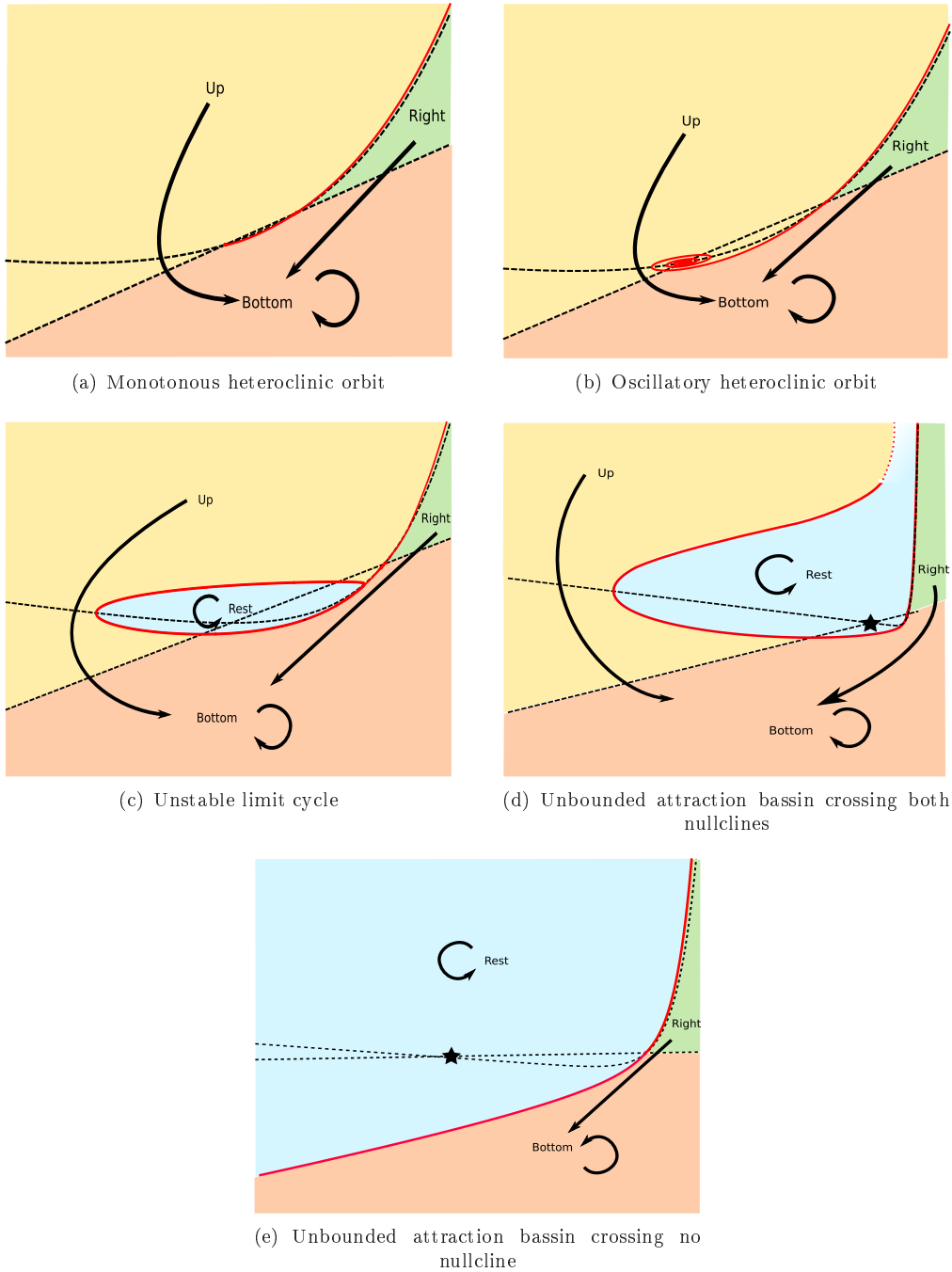


Figure 4: Markov partition of the dynamics: the bottom region is a stable region where each trajectory starting from the up or right region will end up in finite time. The rest region composed of the attraction basin of the possible stable trajectory is an isolated region.

time. Let $w_0 \in \mathcal{D}$, and denote $(v(t), w(t))$ the solution of (1.1) with initial condition (v_r, w_0) and t^* the blowing time of v . The Poincaré map Φ is the unique function such that

$$\Phi(w_0) = w(t^*) + d$$

The Poincaré map gives the next reset location of a spiking trajectory starting on the line $v = v_r$. If we are interested in the spike patterns generated from an initial condition (v_0, w_0) where possibly $v_0 \neq v_r$, the analysis will be valid after the first spike is emitted. More precisely, either (v_0, w_0) is in the attraction basin of a bounded trajectory or on the stable manifold of the saddle fixed point, then it will not elicit a spike. If it is not, then it will fire in finite time and be reset on the line $v = v_r$ at a given level, say w_1 . From this point, the study of the iterations of the map Φ will be valid.

Moreover, assume that in the dynamical system defined by (1.1) starting from the initial condition (v_r, w_0) is in a tonic spiking behavior (i.e. fires after any given time T , hence elicits infinitely many spikes). Then let $(t_n)_{n \geq 0}$ be the sequence of spike times, and define the sequence of adaptation reset points by $w_n := w(t_n) = w(t_n^-) + d$. The Poincaré map of this dynamical system is the function Φ such that

$$\Phi(w_n) = w_{n+1}$$

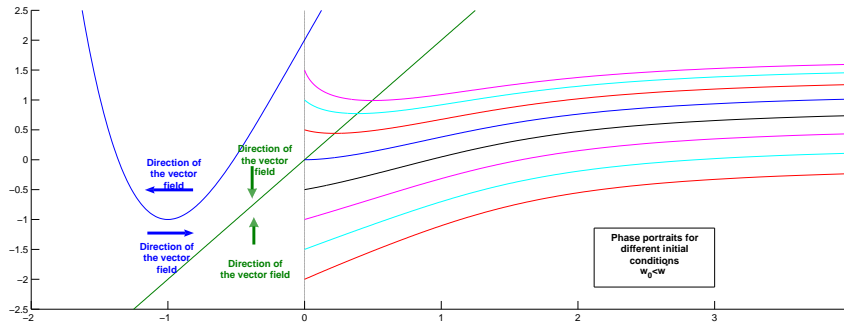
Hence we will be able to apply techniques of nonlinear analysis of iterations of maps to study the spiking location sequences and the spiking times.

For these reasons, we will be interested in the sequel in the dynamics of the iteration of the map Φ which corresponds to a trajectory starting from an initial condition on the line $v = v_r$. On this line, the intersections of the line $v = v_r$ with the nullclines will be of particular interest in the study of Φ . We omit for the sake of simplicity the dependency of these points with respect to the parameters, and define:

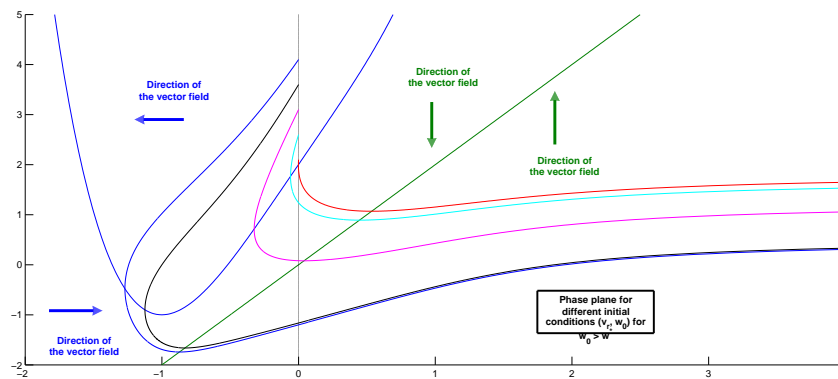
$$\begin{cases} w^* &= F(v_r) + I \\ w^{**} &= bv_r \end{cases} \quad (1.4)$$

Both point depend on the reset voltage v_r . Interestingly enough, besides v_r , the point w^* only depends on the input current and the nonlinearity, while the point w^{**} only depends on the parameter b . The figure Fig.5 represents bundles of trajectories for $w < w^*$ or $w > w^{**}$ in the case where the nullclines do not intersect. It illustrates the qualitative distinctions linked with the relative location of w with respect to w^* .

The time it takes the neuron to elicit a spike governs the inter-spike interval. It is therefore a very pertinent information for a quantitative analysis of the models, or for understanding the neural code. This map, as the Poincaré application Φ , is defined on the spiking domain \mathcal{D} by: $\mathcal{T} : w \mapsto t^*(w)$ where $t^*(w)$ is the spike time if the membrane potential starts at (v_r, w) at time $t = 0$. If this map is one-to-one, then the reset location is directly linked with the interspike interval. Figure Fig.6 represents the map \mathcal{T} in the case of the quartic model for different sets of parameters. We observe that this map is not always injective. Let us describe quickly its dynamics in the case where there is no fixed point for



(a) Phase plane for $w_0 < w^*$



(b) Phase plane for $w_0 > w^*$

Figure 5: Phase plane and trajectories for the quartic model in the no-fixed point case. The trajectories starting from $w < w^{**}$ have an increasing w all along the trajectory, which is not the case for $w > w^{**}$. For $w > w^*$, we observe that the trajectory turns around the point (v_r, w^*) and crosses again the line $v = v_r$ before spiking.

the subthreshold dynamics. In this case, \mathcal{T} is defined for all $w \in \mathbb{R}$, it is increasing for $w \leq w^*$, as a straightforward application of the monotony of the modulus of the vector field with respect to w and the shape of the phase diagram partition in trajectories. For $w > w^*$, the trajectory turns around the point (v_r, w^*) and crosses again the curve $v = v_r$. Here again, it is clear that the time it takes for crossing again the curve $v = v_r$ increases with w . This time increase is compensated by the fact that when w increases, the second crossing

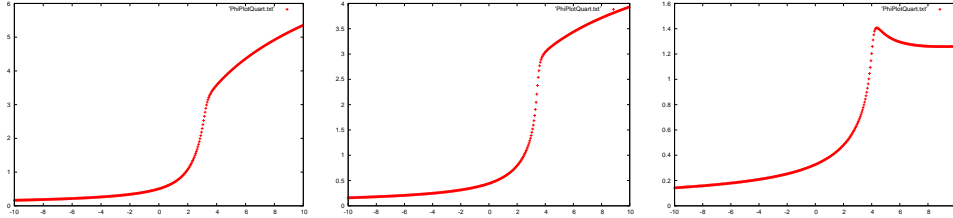


Figure 6: Spike times \mathcal{T} function for the quartic model for different values of a and b . We can see that the function is not always increasing.

location of the curve $v = v_r$ decreases. Eventually, as we prove in the sequel, the second crossing location of the curve $v = v_r$ has a lower bound, and hence after a given time, the map \mathcal{T} will increase again.

As already discussed, the map \mathcal{T} is not always one-to-one. Therefore few reset locations can correspond to the same interspike interval. In this case, if the dynamics of the map Φ does not converge to a fixed point but to a cycle containing two points corresponding to the same spike time could be considered as regular spiking. Nevertheless, it will be considered as a burst of period two both from our mathematical point of view and from the electrophysiological point of view. Indeed, necessarily one of the points w will be associated with a sharp afterpotential (i.e. the membrane potential will be increasing all along the trajectory) and the other with a broad afterpotential (i.e. the membrane potential will first decrease, then increase to the spike), which is characteristic of the bursts.

For these reasons, this map will not be of great interest in our study since we will focus on qualitative properties of the spike sequences, and this map does not perturb the phenomena we consider.

Now that we introduced the main ingredients of our study, we will study the main properties of this map. The different spike patterns are linked with the topology of the domain \mathcal{D} and with properties of the map Φ . We chose here to present our results in function of the subthreshold dynamical properties, since it will make our mathematical analysis clearer. We will summarize the different regions of parameters for which a given spike pattern is produced in section ??.

2 No fixed point case

In this section we consider the case where there is no fixed point in for the subthreshold dynamical system. This case corresponds to the case where $I > -m(b)$ according to theorem 1.2. In that case the system has neither stable fixed point nor limit cycle, and hence no bounded trajectory. The neuron will emit a spike whatever its initial condition. Indeed, let (v_0, w_0) be a given initial condition at time t_0 for the subthreshold system. According to the

diagram 1, the trajectory will always be after a given finite time in the South zone, which corresponds in this case to the bottom zone. As already discussed in section 1.6, as soon as the trajectory enters this zone, it keeps trapped in this zone and blows up in finite time according to Gronwall's theorem.

Therefore, the definition domain of the Poincaré map is $\mathcal{D} = \mathbb{R}$: for any initial condition, the neuron will elicit a spike. Let us now characterize the Poincaré application in this case.

Theorem 2.1. *In the case $I > -m(b)$, the Poincaré map satisfies the following properties (see figure Fig.7):*

- It is increasing on $(-\infty, w^*]$ and decreasing on $[w^*, \infty)$,
- For all $w < w^{**}$ then $\Phi(w) \geq w + d > w$,
- The map Φ is regular,
- It is concave for $w < w^*$,
- It has a unique fixed point in \mathbb{R} ,
- It has an horizontal asymptote (plateau) when $w \rightarrow \infty$

This theorem is quite important to understand the main properties of the reset sequence. These properties are straightforwardly proved if we had a spiking threshold, the only technical intricacy is the fact that the spike occurs when the membrane potential blows up.

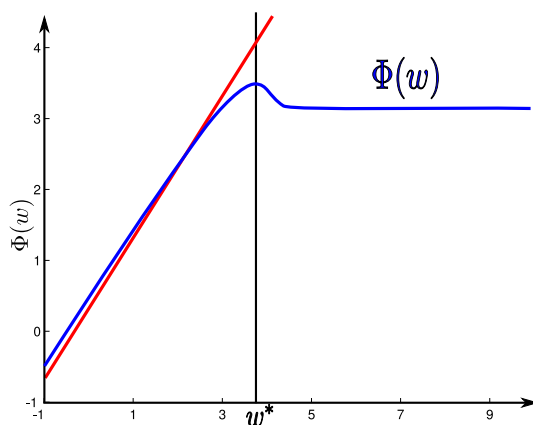


Figure 7: The Poincaré application Φ in the case of the quartic model for $I > -m(b)$ (no-fixed point). The blue line corresponds to the map Φ , the red line to the identity map and the black line localizes w^* . We can observe easily on this diagram the main properties of Φ in this case stated in theorem 2.1.

Proof.

- *Monotony:* Because of Cauchy-Lipchitz existence and uniqueness theorem, two orbits cannot cross between two spike times, since we have uniqueness of the solution for a given initial condition. Let us consider the Jordan section defined by the curve $\{v = v_r\}$. By application of Jordan's theorem (see for instance [4, Chap. 9, appendix, p. 246]), the solutions are always ordered on this section. It means that if $w_1^0 < w_2^0$ and the two solutions cross again the Jordan section, then the order of the new crossing positions w_1^1 and w_2^1 is changed, i.e. $w_2^1 < w_1^1$.

Let $w_1(0) < w_2(0) \leq w^*$ two points in \mathcal{D} . Let $v_1(t)$ and $v_2(t)$ be the solutions of the equations (1.1) with initial conditions $(v_1(0) = v_r, w_1(0))$ and $(v_2(0) = v_r, w_2(0))$ respectively. Then we just have to show that the monotony of the solutions is conserved asymptotically when $v \rightarrow \infty$. This is true because these solutions are in the bottom region and cannot escape from this zone. In this region, the variables $v(t)$ and $w(t)$ are strictly increasing and blow up in finite time. Therefore, the solutions are ordered the same way as the initial condition all along the trajectory and hence $w_1(t_s) \leq w_2(t_s)$ where t_s is the spike time. Hence Φ is increasing on $(-\infty, w^*]$.

Let now $w^* \leq w_1(0) < w_2(0)$. In that case, the initial condition is in the up zone (the "North" zone), and in this zone, the variable v decreases, until crossing the v -nullcline. After crossing this nullcline, the variable $v(t)$ will increase. In will then enter the Center zone and eventually the South (bottom) zone, and blow up in finite time. Therefore, the solutions will cross the Jordan section $\{v = v_r\}$ exactly once, say at time t_r . At this time, the order of the solutions will be inverted ($w_1(t_r) > w_2(t_r)$). Starting from these points, the above analysis applies, and therefore Φ is decreasing on $[w^*, \infty)$.

- *Behavior for $w < w^{**}$:* If $w < w^{**}$, then w will increase all along the trajectory, and hence $w(t_s) \geq w$ and hence $\Phi(w) \geq w + d$.
- *Regularity:* The regularity of Φ for $w < w^*$ comes from the theorem of regularity of the solution of an ordinary differential equation with respect to its initial condition. The equation of the orbits of the system in the phase plane reads:

$$\frac{dw}{dv} = \frac{a(bv - w)}{F(v) - w + I}$$

since in the region $w < w^*$ (South, or bottom region) the value of $F(v) - w + I$ never vanishes (it has the lower bound $I - m(b) > 0$). Let us denote $w(v; v_r, w_0)$ the solution of this differential equation with initial condition w_0 at $v = v_r$. Since the application $(v, w) \mapsto \frac{a(bv - w)}{F(v) - w + I}$ is C^∞ in w , Cauchy-Lipchitz' theorem with parameters [?] implies that the map $(v, v_r, w_0) \mapsto w(v; v_r, w_0)$ is C^∞ . Furthermore, because of assumption (A1), this function has a finite limit when $v \rightarrow \infty$. The regularity of Φ with respect to the initial condition is equivalent to the regularity of the application

$$w_\infty : w_0 \mapsto \lim_{v \rightarrow \infty} w(v; v_r, w_0)$$

To ensure that the map w_∞ is continuous, we need to ensure that the convergence of the applications $w(v; v_r, w_0)$ is uniform (or C^k) when $v \rightarrow \infty$. The differential of the application $w_0 \mapsto$

For $w > w^*$, the orbit will turn around the point (v_r, w^*) . Hence Φ is the composition of the application giving the first crossing location of the orbit with the curve $\{v = v_r\}$ and Φ for $w < w^*$. The second is continuous because of the latter argument, and the first one is clearly continuous. Indeed, we know that at the initial time both w and v will decrease. Fix $w_1 > w_2 > w^*$. Here again, the partition argument and the direction of the vector field ensures us that the position of the new crossing point is continuous with respect to the initial condition.

At the point $w = w^*$, the same argument is still valid, hence our theorem is proved.

- *Concavity:* The solution of equation (1.1) will never cross the v nullcline. Let us write the solution of the orbit curves:

$$\frac{dw}{dv} = g(v, w) := \frac{a(bv - w)}{F(v) - w + I} \quad (2.1)$$

We consider the flow of the dynamical system (2.1) which we denote $\varphi(w_0, v_0, v)$ and we prove the convexity condition on φ :

$$\frac{\partial^2 \varphi}{\partial w_0^2} < 0 \quad \forall (w, v)$$

Indeed, we have:

$$\begin{cases} \frac{\partial g}{\partial w} &= -a \frac{F(v) - bv + I}{(F(v) - w + I)^2} \\ \frac{\partial^2 g}{\partial w^2} &= 2 \frac{bv - F(v) - I}{(F(v) - w + I)^3} \end{cases}$$

and we know that on the trajectory $F(v) - w + I > 0$ and that because of the nullclines positions $bv - F(v) - I < 0$. Hence we have

$$\begin{cases} \frac{\partial g}{\partial w} < 0 \\ \frac{\partial^2 g}{\partial w^2} < 0 \end{cases}$$

Now let us compute the second derivative of φ with respect to w_0 . We have $\varphi(w_0, v_0, v) = w_0 + \int_{v_0}^v g(u, \varphi(w_0, v_0, u)) du$ and hence:

$$\frac{\partial^2 \varphi}{\partial w_0^2} = \int_{v_0}^v \frac{\partial^2 g}{\partial w^2} \left(\frac{\partial \varphi}{\partial w_0} \right)^2 + \frac{\partial g}{\partial w} \frac{\partial^2 \varphi}{\partial w_0^2},$$

and hence we have $\frac{\partial^2 \varphi}{\partial w_0^2} \leq \int_{v_0}^v \frac{\partial g}{\partial w} \frac{\partial^2 \varphi}{\partial w_0^2}$. On the other hand, we can see using this equation that $\frac{\partial^2 \varphi}{\partial w_0^2}(w_0, v_0, v_0) = 0$. Thus using Gronwall's theorem we obtain the convexity of the function $\varphi(\cdot, v_0, v)$ for all v_0 and all v .

The Poincaré application Φ is defined by

$$\Phi(\cdot) = \lim_{v \rightarrow \infty} \varphi(\cdot, v_r, v)$$

and hence Φ has the same convexity property for $w < w^*$.

- *Existence and uniqueness of fixed point:* Let $w_0 < w^*$. Since we have for all $x < w^{**}$ the property: $\Phi(x) \geq x + d$ and for $x > w^*$, $\Phi(x)$ is a non-increasing function, we have existence of at least one fixed point. The uniqueness is given by the concavity of Φ for $w < w^*$ and the decreasing behavior of Φ for $w > w^*$.
- *Horizontal asymptote (plateau) :* The only thing to prove is the existence of a solution diverging to $-\infty$ when $t \rightarrow -\infty$. To do so, we search for an invariant subspace of the phase plane for the inverse dynamics (i.e for the dynamical system $(v(-t), w(-t))$) which does not cross the v nullcline : $\mathcal{N} := \{w = F(v) + I\}$.

For instance, we search for a domain bounded by two lines:

$$\mathcal{B} := \{(v, w) \mid v \leq v_0, w \leq w_0 + \alpha(v - v_0)\}$$

We show that we can find real parameters (v_0, w_0, α) such that this domain is invariant by the dynamics and does not cross \mathcal{N} .

First of all, for the boundary $\{v = v_0, w \leq w_0\}$, we want $\dot{v} \geq 0$, which only means $w \leq w^*(v_0) = F(v_0) + I$.

Now we have to characterize both v_0 , w_0 and α such that the vector field is flowing out of this affine boundary. This simply means that $\langle \begin{pmatrix} \dot{v} \\ \dot{w} \end{pmatrix} | \begin{pmatrix} \alpha \\ -1 \end{pmatrix} \rangle \leq 0$, i.e.: $\alpha \dot{v} - \dot{w} \leq 0$, on each point of the boundary, which is equivalent to:

$$a(bv - w_0 - \alpha(v - v_0)) \geq \alpha(F(v) - w_0 - \alpha(v - v_0) + I) \quad (2.2)$$

Using the assumption $\lim_{v \rightarrow -\infty} F'(v) < 0$, hence there exists an affine function such that for all $v \in \mathbb{R}$ $F(v) + I \geq uv + \beta$.

We consider now $\alpha < 0$. Then condition (2.2) implies that

$$(ab - \alpha(u - \alpha) - a\alpha)v + (-aw_0 + \alpha av_0 + \alpha w_0 - \alpha^2 v_0) \geq 0$$

Hence the only thing to ensure is that $(ab - \alpha(u - \alpha) - a\alpha) < 0$. This condition is achieved when the discriminant of this equation is strictly positive, i.e. for all $u > 2\sqrt{ab} - a$ or $u < -2\sqrt{ab} - a$.

The initial condition on u was to be greater than the minimum of F' , hence any $u > \max(2\sqrt{ab} - a, \min_{v \in \mathbb{R}} F'(v))$ will be convenient, and $\alpha = \frac{a+u}{2}$.

In this case, for all $v < v_m$ and $w_0 < w_u$ the intersection of $\{v = v_m\}$ and the tangent at F at the point x_u solution of $F'(x_u) = u$, the vector field is flowing out \mathcal{D} and hence when we invert the time direction, the vector field is flowing in this zone, hence \mathcal{D} is flow invariant, hence every solution in this zone does not cross the nullcline, hence goes to infinity with a speed minored by the minimal distance between the nullcline and \mathcal{D} .

Hence we have proved that there is a solution going to $-\infty$, and which will spike by assumption. This solution crosses necessarily the line $\{v = v_r\}$, and denote w_L the w associated to this intersection. This solution cuts the phase space in two subspaces which do not communicate: every orbit starting in one of the two subspaces will stay in this subspace. Hence for all $w > w^*$, $\Phi(w) \geq \Phi(w_L)$, hence Φ is decreasing and minored, hence converges to a certain value.

□

2.0.1 Case of two unstable fixed point and no stable limit cycle

In this case, the structure of the stable manifold of the saddle fixed point is very important to understand the dynamics. Because of the properties of the subthreshold dynamics, it is easy to show that in this case the stable manifold of the saddle fixed point connects to the unstable fixed point, since any trajectory outside the stable manifold will elicit a spike. This manifold will possibly wind around the saddle fixed point if the eigenvalues of the unstable fixed point have a non-null imaginary part (see Fig.8(a)). For instance this will be the case around the Hopf bifurcation. At each crossing point of the line $v = v_r$ with this stable manifold, the map Φ is undefined. The nature of the trajectories before and after these intersections completely changes, and at this point the map Φ undergoes jumps. Hence when the stable manifold oscillates around the fixed point, the map Φ will have arbitrary many discontinuity points.

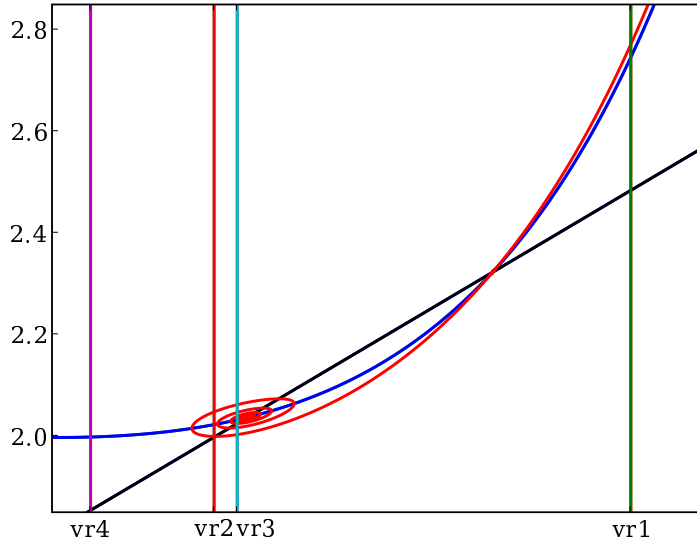
On the subsets where the map Φ is defined, it is regular, continuous, increasing for $w < w^*$ and decreasing for $w > w^*$, for the same reasons as in the case ??.

If $v_r > v_+$ then the map Φ will have a unique discontinuity, and whenever $v_r > v_-$, the map Φ will have an even number of discontinuities. For $v_r < v_-$, the map Φ will possibly have an odd number of discontinuity points. Finally, there exists a certain value V_{\min} of the potential such that the stable manifold is completely contained in the set $\{v > v_{\min}\}$. For any $v < V_{\min}$ the map Φ is continuous.

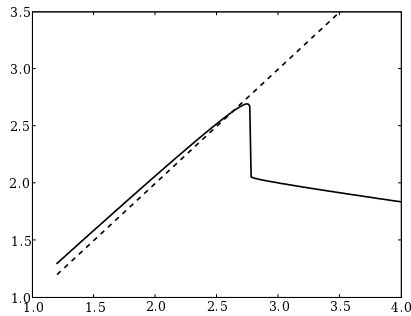
The diagram 8 represents this dichotomy in the case of the dimensioned adaptive exponential model, for the set of parameters used for figure 8(a)

2.0.2 Existence of stable bounded trajectories

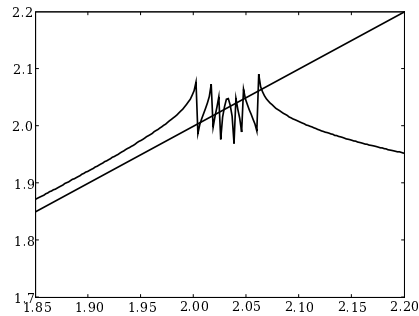
The bounded trajectories in this class of models can be either fixed points or a stable periodic orbits. A point (v, w) belongs to the attraction basin of a stable trajectory if and only if



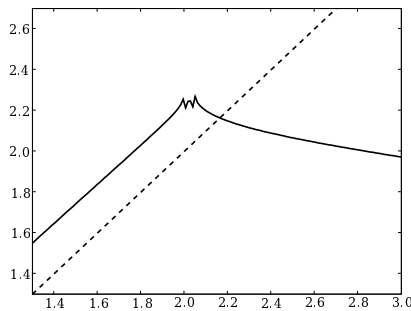
(a) Nullclines and different reset locations $v_{r1}, v_{r2}, v_{r3}, v_{r4}$ corresponding to different qualitative behaviors for the map Φ .



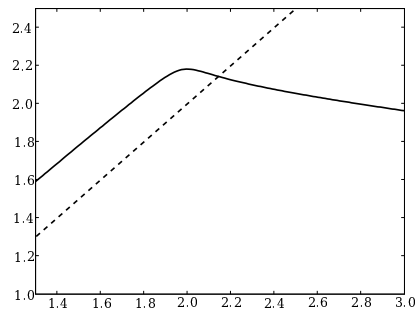
(b) $v_r = v_{r1}$: 1 discontinuity point



(c) $v_r = v_{r3}$: 6 discontinuity point, 7 fixed points



(d) $v_r = v_{r2}$: 2 discontinuity point



(e) $v_r = v_{r4}$: Φ is continuous

INRIA

Figure 8: Case of two unstable fixed points for the classical adaptive exponential model. Phase plane and graph of the map Φ for different values of v_r , for the same set of parameters, except for the case 8(e) where we changed the usual spike-triggered adaptation parameter, to show that in the case of two unstable fixed points the map Φ can have many fixed points.

the system (1.1) starting from this point converges towards this trajectory. The topology of this set is governed by the subthreshold dynamics. The problem of identifying in a closed form the attraction basin of the bounded solutions is very hard to handle formally. In the present paper we describe qualitatively these sets and then compute them numerically using continuation algorithms. The study of the attraction basins of bounded trajectories requires to study in details the subthreshold dynamics. It appears that the attraction basins of the stable trajectories are linked with the shape of the stable manifold of the saddle fixed point. This precise analysis is derived in the appendix ???. From this analysis, it appears that two main types of topologies can appear for the attraction basins of the bounded trajectories:

1. In the case of the attracting cycle or of the stable fixed point after the saddle-homoclinic bifurcation (i.e. when the family of unstable limit cycle originated from the Hopf bifurcation exists), the boundary of the attraction basin is unbounded. In this case, we can distinguish the case where the separatrix crosses the v -nullcline or not. In the case where the limit at $-\infty$ of F is bounded, then we can find a condition for the crossing of the v -nullcline but in the general case, we cannot tell whether if the nullcline will cross the v nullcline or not.
2. In the case of a stable fixed point circled by an unstable limit cycle originated from the Hopf bifurcation, the attraction basin is bounded by this unstable cycle.

In the case where the nonlinear function F satisfies $F'''(v_a) < 0$ for v_a the unique solution of $F'(v_a) = a$, then the system undergoes a Bautin bifurcation and the subcritical Hopf bifurcation becomes supercritical, generating an attracting limit cycle corresponding to self-sustained subthreshold oscillations. In this case, there is no fixed point, but the attracting limit cycle is a bounded trajectory and doesn't leads to a spike. As stated, the domain \mathcal{D} is no more necessarily the whole real line \mathbb{R} . If we denote by \mathcal{A} the attraction domain of the bounded solutions, the definition domain of Φ is simply $\mathbb{R} \setminus \mathcal{A}$.

In this case, as stated in section ??, the attraction basin is unbounded. It can either cross the v nullcline, and in this case the attraction basin has a lower voltage bound v_{\min} , or not.

If the separatrix crosses the v -nullcline, then for $v_r < v_{\min}$, $\mathcal{D} = \mathbb{R}$ and the map Φ has exactly the same shape as described in the no fixed point case treated in section ??. If $v > v_{\min}$, then $\mathcal{D} = (-\infty, w_{\min}(v_r) \cup (w_{\max}(v_r), \infty)$. For $v_r < v_+$, the map Φ is regular, increasing and concave on the first interval, and on the second one it is regular and decreasing. For $v > v_+$, then $w_{\min}(v_r) > w^* > w^{**}$. In the interval $(-\infty, w_{\min}(v_r))$, the map Φ is regular, increasing and concave for $w < w^*$, greater than $id + d$ (where id is the identity map) for $w < w^{**}$ and decreasing for $w^* < w < w_{\min}(v_r)$. On the interval $(w_{\max}(v_r), \infty)$, it is regular, decreasing, and has a horizontal asymptote for $w \rightarrow \infty$.

If the separatrix does not cross the v -nullcline, then it is unbounded in voltage, and hence the definition domain \mathcal{D} is of the type $(-\infty, w_{\min}(v_r))$. If $v_r < v_+$ then the map Φ is increasing, regular and concave on \mathcal{D} . If $v_r > v_+$, then $w_{\min}(v_r) > w^* > w^{**}$, and the map Φ is regular, concave and increasing for $w < w^*$, greater than $(id + d)$ for $w < w^{**}$, and regularly decreasing for $w^* < w < w_{\min}(v_r)$.

2.0.3 Existence of a stable fixed point

In the case where there exists a stable fixed point for the subthreshold dynamics, the attraction basin can be either bounded or unbounded. In the latter case, the definition domain and the dynamics of Φ is exactly the same as described in the case where there exists a stable limit cycle (section ??).

In the case where the attraction basin of the stable fixed point is bounded, let us denote by $v_{\min, \mathcal{D}}$ and $v_{\max, \mathcal{D}}$ the bounds of this domain in the v variable, and $\{w_{\min}(v_r), w_{\max}(v_r)\}$ the bounds of \mathcal{D} for a given $v_r \in (v_{\min, \mathcal{D}}, v_{\max, \mathcal{D}})$.

If $v < v_{\min, \mathcal{D}}$, then $\mathcal{D} = \mathbb{R}$ and the map Φ has the same characteristics as in the case where there is no fixed point (see section ??). If $v > v_{\max, \mathcal{D}}$, then the domain \mathcal{D} is equal to \mathbb{R} deprived of the intersection of the stable manifold of the saddle fixed point with the line $v = v_r$. In this case, the shape of Φ is the same as in the case where there are two unstable fixed points (see section 2.0.1), and in particular it has a discontinuity at $w = w^*$.

Eventually, for $v_{\min, \mathcal{D}} < v_r < v_{\max, \mathcal{D}}$, the domain \mathcal{D} is composed of two subintervals $(-\infty, w_{\min}(v_r))$ and $(w_{\min}(v_r), \infty)$, and the dynamics of Φ on this set is the same as described in the case where there exists a stable limit cycle whose attraction basin crosses the v -nullcline (see section ??).

3 Phasic Behaviors

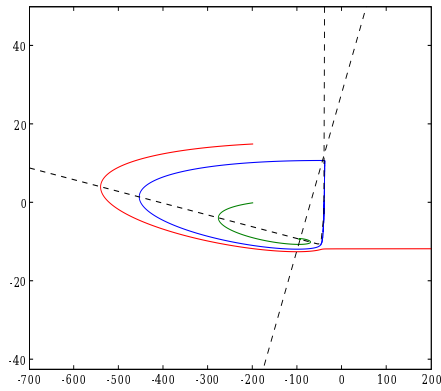
In this section, we consider the cases where the neuron has a phasic spiking behavior. In this case necessarily, after a given possibly spiking transient phase, the system is attracted towards a bounded trajectory, either a fixed point or a stable limit cycle. This section is aimed to explain qualitatively the origin of some of the phasic behaviors observed in the papers [1, 9, 19] in the framework we introduce in the present paper.

Hence the cases we consider here are the cases introduced in sections ?? and 2.0.3. As we have seen in these sections, the attraction basin of the stable periodic orbit is unbounded, and the attraction basin of the fixed point can be either bounded or unbounded. We will distinguish in this study two cases: the first case is the case where the boundary of the attraction is an increasing function of v (i.e. necessarily in the case where the attraction basin is unbounded), and the case where it crosses both nullclines.

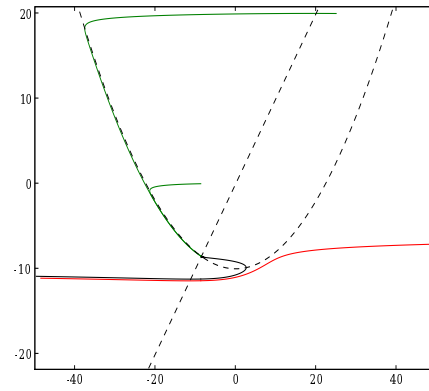
3.1 Unbounded increasing separatrix

In the cases where the attraction basin of the fixed point is unbounded and an increasing function of v , then the definition domain of the map Φ is always of type $(-\infty, w_{\min, \mathcal{D}}(v_r))$. In this case, phasic behaviors only occur when $\Phi(w_{\min, \mathcal{D}}(v_r)) > w_{\min, \mathcal{D}}(v_r)$. In this case, we have $\Phi(w) \geq w + \varepsilon$ for some $\varepsilon > 0$. Hence for any $w \in \mathcal{D}$, there exists $n \in \mathbb{N}^*$ such that $\Phi^n(w) > w_{\min, \mathcal{D}}(v_r)$ and hence $\Phi^n(w) \notin \mathcal{D}$. The neuron will send n spikes and then is attracted by the bounded trajectory and will not spike anymore.

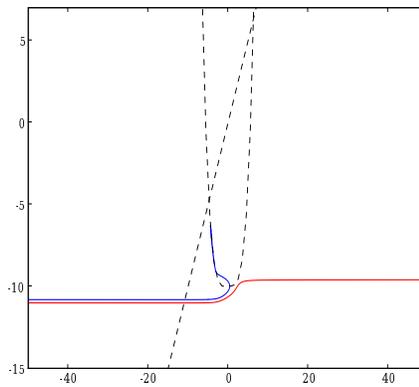
In the case where $\Phi(w_{\min, \mathcal{D}}(v_r)) < w_{\min, \mathcal{D}}(v_r)$, then there exists a unique fixed point for the map Φ . We distinguish two cases:



(a) Exponential Model



(b) Quadratic Model



(c) Quartic Model

Figure 9: Attraction Basin of the stable fixed point in the case of the exponential, the quadratic and the quartic adaptive neuron models. We represented in red the lowest spiking trajectory.

- if $v_r < v_+$, then the map Φ is increasing on \mathcal{D} , $\Phi(\mathcal{D}) \subset \mathcal{D}$ and hence the neuron will not be in a tonic spiking case.
- if $v_r > v_+$, then the map Φ is increasing on $(-\infty, w^*(v_r)]$ and decreasing on $[w^*(v_r), w_{\min, \mathcal{D}}(v_r))$. If $\max_{x \in \mathcal{D}} \Phi(x) < w_{\min, \mathcal{D}}(v_r)$ then the neuron is always in a tonic behavior, since $\Phi(\mathcal{D}) \subset \mathcal{D}$. If it is not the case, then there exists a non-empty domain \mathcal{A}_1 such that $\Phi(x) \notin \mathcal{D}$ for all $x \in \mathcal{A}_1$. For any initial condition w in \mathcal{A}_1 , the neuron will send a spike and then return to equilibrium. By an immediate induction, we define $\mathcal{A}_{n+1} = \Phi^{-1}(\mathcal{A}_n)$ the set of initial conditions such that the neuron emits exactly n spikes before returning to equilibrium. The set of phasic spiking initial conditions is hence $\cup_{n=1}^{\infty} \mathcal{A}_n$ and the set of tonic spiking initial condition its complementary. This set is a union of intervals. Let us describe this set a little bit further. The set \mathcal{A}_1 is equal to $\Phi^{-1}(\mathcal{A})$ where \mathcal{A} is the attraction basin of the bounded trajectory. It corresponds to the points such that $\Phi(w) > w_{\min, \mathcal{D}}(v_r)$. Hence it is an interval $[a_1^1, a_2^1]$ with $a_1^1 < w^* < a_2^1 < w_{\min, \mathcal{D}}(v_r)$. The set \mathcal{A}_2 is the reciprocal image of \mathcal{A}_1 under Φ . This phasic spiking set will never cover completely \mathcal{D} . Indeed, the fixed point of Φ , which we denote w_f , is a tonic spiking point. Furthermore, if the fixed point w_f is stable ($|\Phi'(w_f)| < 1$), then there exists an interval \mathcal{T}_1 such that $\Phi(\mathcal{T}_1) \subset \mathcal{T}_1$ and hence the spiking set will be a reunion of non-empty intervals. If the fixed point is unstable, then the set of transient dynamics is $\mathcal{D} \setminus \{w_f\}$.

3.2 Bounded or turning separatrix

In this section we consider the cases where the boundary of the attraction is either a limit cycle or crosses both nullclines.

As already discussed, in these cases, the domain \mathcal{D} is either \mathbb{R} or a union of two unbounded intervals. The case where $\mathcal{D} = \mathbb{R}$ is always a tonic spiking case, and hence will be treated in the section dedicated to these behaviors. We hence consider here the case where the domain \mathcal{D} is the union of two interval $\mathcal{D} = (-\infty, w_{\min, \mathcal{D}}(v_r)) \cup (w_{\max, \mathcal{D}}(v_r), \infty)$. We first note that $\Phi((w_{\max, \mathcal{D}}(v_r), \infty)) \subset \Phi((-\infty, w_{\min, \mathcal{D}}(v_r)))$ because of the properties of the sub-threshold dynamics. Indeed, any trajectory starting from (v_r, w) with $w \in (w_{\max, \mathcal{D}}(v_r), \infty)$ will cross the line $v = v_r$ at some point $w \in (w_{\max, \mathcal{D}}(v_r), \infty)$. Hence we focus in the sequel on the dynamics of Φ on $I_1 := (-\infty, w_{\min, \mathcal{D}}(v_r))$.

On this interval, if $\max_{x \in I_1} \Phi(x) < w_{\min, \mathcal{D}}(v_r)$, then the system will never escape from \mathcal{D} and hence will be in a tonic spiking behavior. There will be phasic spiking if $\max_{x \in I_1} \Phi(x) < w_{\min, \mathcal{D}}(v_r)$.

For instance, if $w_{\min, \mathcal{D}}(v_r) < \Phi(w_{\min, \mathcal{D}}(v_r))$ and $w_{\min, \mathcal{D}}(v_r) < \max_{x \in I_1} \Phi(x) < w_{\max, \mathcal{D}}(v_r)$, then the system will be unconditionally transient, i.e. for any $w \in \mathcal{D}$, there exists $n \in \mathbb{N}^*$ such that $\Phi^n(w) \notin \mathcal{D}$. Indeed, the sequence $\Phi^k(w)$ is strictly increasing and will end up in $\mathbb{R} \setminus \mathcal{D}$ after a given number of iterations.

If $w_{\min, \mathcal{D}}(v_r) > \Phi(w_{\min, \mathcal{D}}(v_r))$ and $w_{\min, \mathcal{D}}(v_r) < \max_{x \in I_1} \Phi(x) < w_{\max, \mathcal{D}}(v_r)$, then the system has a stable fixed point, and hence there exists a subset of \mathcal{D} stable under Φ (since the dynamics is contracting in the neighborhood of the fixed point). In this case again,

the transient behavior set will be a countable union of intervals as in the case previously described.

A more complex structure will appear if $\max_{x \in I_1} \Phi(x) > w_{\max, \mathcal{D}}(v_r)$. In this case, ...

3.3 Phasic behaviors

Many authors described two main types of phasic behaviors : phasic spiking and phasic bursting. It appears that in terms of dynamics, the only difference one can do between two phasic behaviors is the number of spikes before returning to equilibrium. In fact, when considering more precisely the traces given by the authors, we observe that the behaviors qualified of phasic bursting only differ from the ones qualified of phasic spiking by the frequency of spike emission, but never present a sequence of bursts followed by a return to equilibrium. Indeed, as we will prove in the tonic spiking section, the bursting corresponds to the convergence towards a stable spiking trajectory. The frequency of spikes is governed by the different time scales and the nonlinearity.

In the classification of these articles, the phasic spiking corresponds to the emission of a single spike, hence to all the set of trajectory crossing the line $v = v_r$ in the set \mathcal{A}_1 . Any other transient dynamics is considered as phasic bursting.

4 Tonic Behaviors

In this section we are interested in what we call the *tonic* behaviors, characterized by the emission of infinitely many spikes. This will be the case whenever $\Phi(\mathcal{D}) \subset \mathcal{D}$, for instance when $\mathcal{D} = \mathbb{R}$ i.e. when there is no stable bounded trajectory (fixed point, periodic orbit) in the subthreshold dynamical system.

We will first treat the case where there is no fixed point in the subthreshold dynamics.

4.1 No fixed point case

In this section, we consider the case where $I > -m(b)$, i.e. when the nullcline do not intersect and hence when there is no fixed point. In this case, the system will always be in a tonic behavior, the domain \mathcal{D} is the whole real line \mathbb{R} and the map Φ has the properties described in section ???. The study of the iterations of Φ will hence give us a good way to understand the different tonic spiking patterns observed in these models.

4.1.1 Tonic spiking

In the article [19], the author observed numerically the existence of a generalized limit cycle, which he called spiking limit cycle, virtually containing a point at infinity (see Fig. 10).

The regular spiking behavior, whatever the phasic behavior, is linked with the presence of such a cycle. This cycle described is exactly a fixed point of the Poincaré application Φ , and the convergence to a regular spiking behavior is simply linked with the convergence of the reset location sequence to this fixed point.

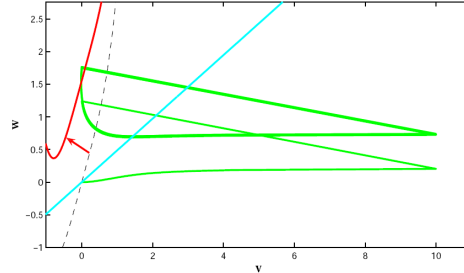


Figure 10: Spiking generalized limit cycle. In the simulation, we have cut the trajectories to a given threshold. At this threshold, we are sure that the solution will blow up, and the trajectory is almost horizontal, hence the real picture is very similar

A simple sufficient condition to get these two conditions is given by the following theorem.

Theorem 4.1. *Assume that $\Phi(w^*) \leq w^*$. Then the sequence of reset positions $(w_n)_{n \geq 0}$ will converge whatever the initial condition.*

Proof. First of all, we deal with the case $w_0 \leq w^*$. The sequence $(w_n)_{n \geq 0}$ is monotonous since we have Φ increasing on $(-\infty, w^*]$. Indeed, assume that $\Phi(w) \leq w$, then by induction on n we have

$$\Phi^{n+1}(w) \leq \Phi^n(w)$$

and hence the sequence is non-increasing. If $\Phi(w) \geq w$, the same argument gives us that the sequence $(w_n)_n$ is non-decreasing.

Note that in this case, we necessarily have $w^{**} < w^*$. Indeed, if it was not the case, then proposition ?? would imply that $\Phi(w) > w$ which contradicts the hypothesis of the theorem.

If $w \in [w^{**}, w^*]$, then we know by the hypothesis of the theorem and by the result of the proposition ?? that this interval is invariant under Φ , and hence $(w_n)_n$ is a monotonous sequence in a compact set, and hence will necessarily converge to a fixed point in $[w^{**}, w^*]$.

If $w < w^{**}$ then $\Phi(w) \geq w + d$ and hence there exists an index N such that $w_N \geq w^{**}$. We apply the result previously proved to obtain that $(w_n)_n$ converges to a fixed point in $[w^{**}, w^*]$.

If $w > w^*$, then Φ is decreasing on this interval, and hence $\Phi(w) \leq \Phi(w^*) \leq w^*$, hence we can use the previous analysis to prove that the system will converge to a fixed point in $[w^{**}, w^*]$. \square

Remark 1. This result implies the property of regular spiking we observed in numerical simulations. This would corresponds by analogy to the conductance based models to a *generalized attracting spiking limit cycle*, generalized because containing a spike in the class of modeled of interest means containing a point $(v = \infty, w)$ for some w .

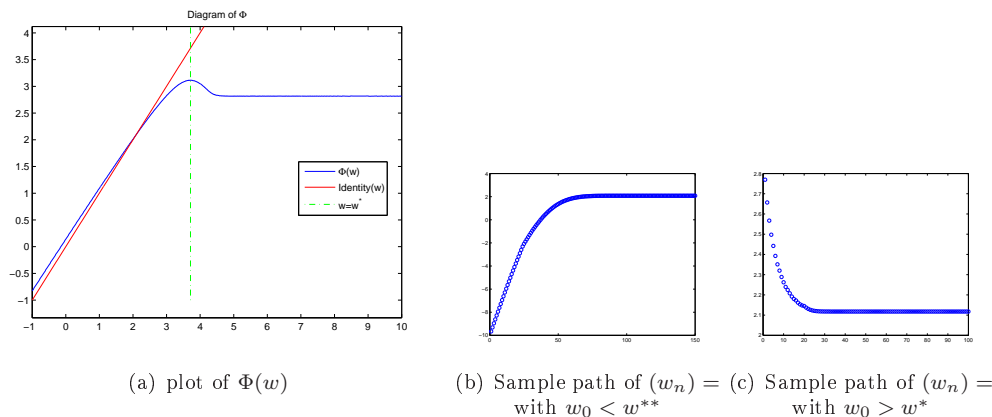


Figure 11: Convergence towards fixed point.

Note that the regular spiking behavior is linked with the convergence of the sequence $(w_n)_{n \geq 0}$. Indeed, if this sequence converges, then the frequency of the spikes will converge also. If it does not, the only way to have regular spiking is to have a cycle and each point of the cycle corresponds to the same spike time in the case where the map \mathcal{T} is not one-to-one. When this case occurs, then one of the point of the cycle is lower than w^* and hence corresponds to a sharp after-potential and the other point is greater than w^* and corresponds to a broad after potential, and the sequence will then be considered as a regular bursting.

The following theorem gives us another sufficient condition on the dynamics to get regular spiking.

Theorem 4.2. *Assume that $\Phi(w^*) > w^*$ and $\Phi^2(w^*) > w^*$. Then the sequence of reset positions will converge to a fixed point whatever the initial condition.*

Proof. First of all, we already noted that there exists a unique fixed point for the map Φ and that this fixed point is in $[w^*, \Phi(w^*)]$. If we have

$$w^* < \Phi^2(w^*) < \Phi(w^*)$$

Then because of the monotony of Φ on (w^*, ∞) , we have (by induction) for all $n \geq 1$:

$$\begin{aligned} \Phi^{2n}(w^*) &< \Phi^{2n+1}(w^*) < \Phi^{2n-1}(w^*) \\ \Phi^{2n}(w^*) &< \Phi^{2n+2}(w^*) < \Phi^{2n+1}(w^*) \end{aligned}$$

Hence the sequence $(w_{2n})_{n \geq 0}$ is an increasing sequence and $(w_{2n+1})_{n \geq 1}$ is decreasing, and for all n , we have $w_{2n} < w_{2n+1}$. Hence the two sequences converge.

We know that because of the monotony conditions on Φ and the plateau that Φ^2 has either a unique fixed point (the same as Φ) or three fixed points. Let $w_1 := \min\{\Phi^{-1}(w^*)\}$. Then Φ^2 is increasing on $(-\infty, w_1)$, decreasing on (w_1, w^*) and increasing again on (w^*, ∞) , and converges to a finite limit when $w \rightarrow \infty$. On $(-\infty, w^*)$, $\Phi^2(w) > w$ because it is clearly the case on $(-\infty, w_1)$ and the minimum of Φ^2 is reached at w^* where $\Phi^2(w^*) > w^*$, hence Φ^2 has a unique fixed point, which is the same as Φ .

Thus the two sequences converge to this same fixed point.

Let now w_0 be an initial condition. Then necessarily the sequence w_n will be in the invariant interval $[w^*, \Phi(w^*)]$. Indeed, assume that $w_0 < w^*$. Then we know that the sequence will not be bounded by w^* , since there is no fixed point in $(-\infty, w^*)$. Hence there will be an integer p such that $\Phi^p(w_0) \leq w^*$ and $\Phi^{p+1}(w_0) \geq w^*$. Then because of the monotony of Φ we have $\Phi^{p+1}(w_0) \leq \Phi(w^*)$. \square

Interestingly enough, the input current has a stabilizing effect on the behavior of the neuron. We can even prove that for I large enough the sequence will always converge to a fixed point. Nevertheless, the complexity we described in the previous sections will clearly affect the dynamics when we vary I . Note that this type of behavior is what is sometimes called fast spiking behavior: it is a case where the neuron fires very fast.

Proposition 4.3. Let a, b, v_r, d be fixed parameters. There exists I_s such that for all $I > I_s$ the sequence of iterates of Φ converges.

Proof. Indeed, consider the point $w^*(I)$ and let I increase. From this point $w^*(I)$, the vector field in the direction of v does not change, and in the direction of the adaptation variable w , it decreases linearly (i.e. increasing I by δI amounts adding $-\delta I$ to the vector field in the direction of w). This new dynamical system can be deduced from the original one changing w in $\tilde{w} = w - I$.

The trajectories are ordered and the order decreases with I . Indeed, let $I_1 < I_2$. The equation of the trajectory reads:

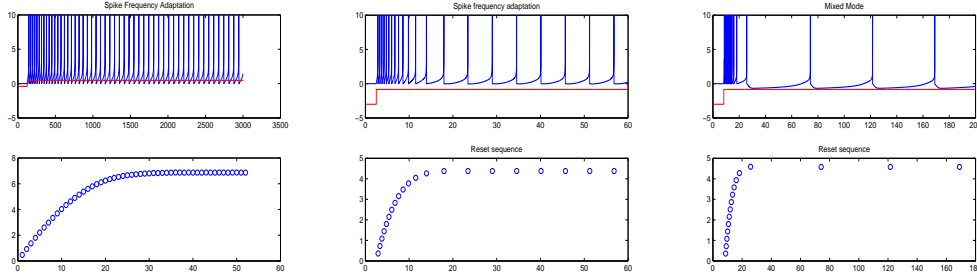
$$\frac{d\tilde{w}}{dv} = \frac{a(bv - w) - aI}{F(v) - w}$$

and hence is decreasing with I . Furthermore, at the point $\tilde{w}^* = F(v_r)$, the vector field is vertical and the amplitude of the vector field increases with I . Hence all the trajectories are ordered, and $\Phi(w^*) - I$ is decreasing with I . Moreover, the trajectories are diverging, i.e. the distance between two trajectories increase with time.

Finally, it is clear that the trajectory in w is not bounded at the beginning of the evolution. Indeed, the vector field at the initial instant is vertical and its amplitude tends to $-\infty$ when $I \rightarrow \infty$.

This can be proved easily by a reductio ad absurdum proof. Assume that \tilde{w} had a lower bound w_{inf} for any I . Then in this case, we would have:

$$\dot{v} = F(v) - \tilde{w} \leq F(v) - w_1 \tag{4.1}$$



(a) Spike Frequency Adaptation (multiplier 0.355) (b) Intermediate case (multiplier 0.068) (c) Mixed Mode (multiplier 10^{-4})

Figure 12: Different types of convergence for the quartic model, when all the parameters are fixed but the time scale of the adaptation variable a . The faster the adaptation is, the slower the convergence is.

and hence $v(t) \leq v_1(t)$ the solution of this equation. This equation do not depend on I . Let dt be a finite time smaller than the explosion time of the equation (4.1) such that for $t \in [0, dt]$, $v(t) \leq v_1$ a given value $\geq v_r$. Then we have for I large enough:

$$\begin{cases} a(bv - w) - aI \leq a(bv_1 - w_1) - aI \leq 0 \\ 0 \leq F(v) - w \leq F(v) - w_1 \\ -\frac{dw}{dv} = -\frac{a(bv-w)-aI}{F(v)-w} \geq \frac{-a(bv_1-w_1)+aI}{F(v)-w_1} \end{cases}$$

This is not possible since for $v \in [v_r, v_1]$, when I increases, w will be as small as one wants. \square

Hence we have to simple criteria for regular spiking. Moreover, we have proved that for an input current large enough, the neuron will spike regularly. Nevertheless, this analysis doesn't distinguishes the simple tonic spiking from the mixed mode or the spike frequency adaptation. The differences between these behaviors is only the transient phase of spiking, which corresponds from a mathematical point of view to the way the sequence of iterates converges towards the fixed point (see Fig.12). From the biological point of view, the distinction between these behaviors is not so clear either. In our framework, we can quantify the convergence speed, which is directly linked with the multiplier of the fixed point. If the modulus of this multiplier is very small (close to 0), then the convergence will be very fast, and we will see a short transient before the regular spiking, and hence we will have a mixed mode (see Fig. 12(c)). If the multiplier modulus is close to 1, then the convergence will be very slow, and we will have spike frequency adaptation (see Fig. 12(a)).

4.1.2 Tonic Bursting

In the numerical analysis of the paper [19], the author observed that bursting activity was linked with the existence of an attracting generalized limit cycle, which he called bursting limit cycle, virtually containing many points having an infinite membrane potential (see Fig. 13). The regular bursting behavior, whatever the transient behavior, is linked with the presence of such a cycle, and this cycle corresponds exactly to periodic points for the the Poincaré map Φ .

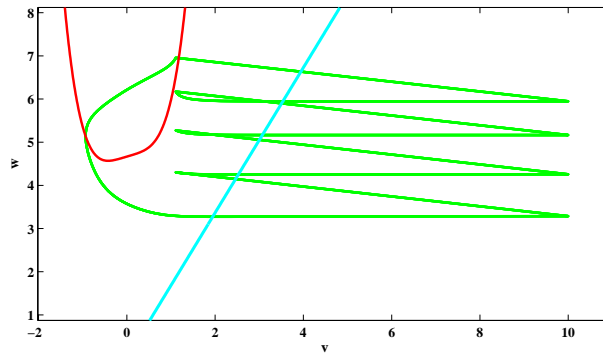


Figure 13: Bursting generalized limit cycle. In the simulation, we have cut the trajectories to a given threshold. At this threshold, we are sure that the solution will blow up, and the trajectory is almost horizontal, hence the real picture is very similar

We can prove that there exists cycles of any period. Indeed, one of the simplest application of Sarkovskii's theorem (see e.g. [3]) is that if there exist a periodic point of period 3, then there exist periodic points of any period, hence bursts of any period. Theorem 4.4 gives us a simple criterion on the dynamics of Φ to have a period 3 cycle.

Theorem 4.4 (Cycles of any period). *Let $w_1 := \min\{\Phi^{-1}(w^*)\}$. Assume that:*

$$\begin{cases} \Phi(w^*) > w^* \\ \Phi^2(w^*) < w_1 \\ \Phi^3(w^*) > w^* \end{cases} \quad (4.2)$$

Then there exists a non-trivial period 3 cycle, hence the reset process has cycles of any period.

Proof. The only thing to prove is that there exist a real T such that

$$\begin{cases} \Phi^3(T) = T \\ \Phi(T) \neq T \end{cases}$$

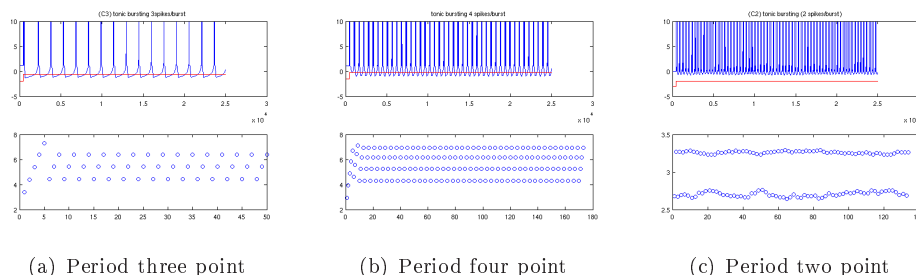


Figure 14: Different types of bursts and the periodic orbits of Φ associated. The last example of a point of period two shows that the system is quite excitable. Indeed, the precision of our integration scheme is very high in this case. This irregularity we observe is linked with numerical errors associated with the excitability of the system: we are very close of the disappearance of this cycle.

We know that there exists a unique fixed point of Φ , which we denote w_∞ and which lies in the interval $[w^*, \Phi(w^*)]$. Here we prove that there exists another solution of $\Phi^3(x) = x$. Indeed, let us describe the function Φ^3 :

- It is increasing on $(-\infty, w_2)$ where $w_2 = \min\{\Phi^{-2}(w^*)\}$, and above the curve $y = x$ on this interval.
- decreasing on (w_2, w_1) and $\Phi^3(w_1) = \Phi^2(w^*) < w_1$ hence the curve crosses once the curve $y = x$, at a point strictly inferior to w^* .

Hence we have proved that there exists a period 3 cycle. Sarkovskii's theorem (see e.g. [3]) ensures us that there are cycles of any period for the map Φ . □

Remark 2. This theorem gives us a quite simple condition on Φ to get period 3 cycles. This implies that the system is chaotic, as shown in the excellent paper of Li and Yorke [14]. Nevertheless the chaos they find is a topological chaos. It means that the set of cycles is dense. It does not corresponds to the usual definition of chaos used in neuroscience, understood as sensitive dependency on initial conditions.

We can easily find in our applications periodic points of period 3, when v_r varies. We can also find experimentally periodic points of different periods, as shown in figure 14.

4.1.3 Bifurcations and Chaos

Now we have seen that varying parameters can change the behavior of the sequence of iterates, from the convergence to a single point to the convergence towards cycles. Hence a

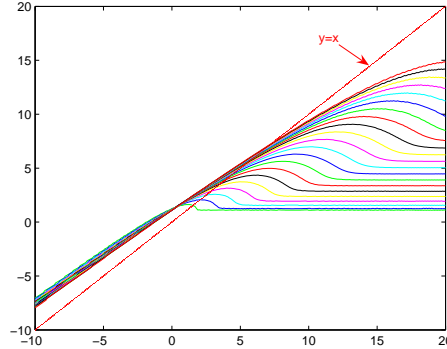


Figure 15: Poincaré application for the quartic model with $a = 1$, $b = 0.5$, $v_r = 3$, $d = 1$ and I ranging from 1 to 20.

natural question arises: how does the behavior of the sequence of iterates depend upon the parameters.

To understand better the transition between these different types of behaviors, it is important to understand better the dependency of the Poincaré map Φ in function of the parameters. The parameter having the simplest effect on the dynamics is the adaptation parameter d which only shifts the Poincaré map. Hence when d is very small, the fixed point will be attractive with a positive multiplier. When d will be very large, then the fixed point will be attractive with a negative multiplier, close to 0 (the fixed point will be on the flat region corresponding to the horizontal asymptote).

As we have already seen, when I increases, after a certain value of I , the sequence will converge towards a fixed point. Increasing I has the effect of linearly translating the point $w^* = F(v_r) + I$, inducing a smooth change of the curve Φ (see figure Fig.15).

The behaviors with respect to these two parameters are hence quite regular. When d is big or I is big, then we have regular spiking.

The dependency in the parameters a and b are also very smooth and monotonous. The map Φ hardly depends on b and the dependency in a is similar to the dependency in I . Figure 16 represents many curves for the same parameters, when varying the parameters a and b .

4.1.4 Bifurcations with respect to the spike-triggered adaptation

As we already showed, the map Φ becomes very sharp when v_r increases. Hence for a certain value of v_r , the minimum of the derivative of Φ will be lower than -1 . Changing the spike-triggered adaptation parameter d amounts shifting the map Φ vertically. Hence increasing b will shift the fixed point along the curve Φ . Assume that for $d = 0$ the fixed point is stable

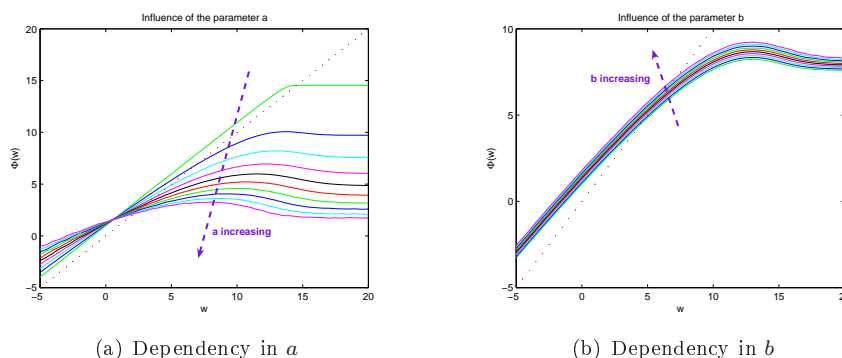


Figure 16: Dependency of the application Φ on the parameters a and b of the subthreshold dynamics.

and lower than the point where the differential of Φ is lower than one. Then the fixed point of Φ will be stable when increasing d until it reaches the first point where the differential of Φ is lower than -1 . At this point the system undergoes a period-doubling bifurcation (the non-degeneracy condition can be easily checked numerically) and hence the sequence of iterates bifurcates from the convergence towards a fixed point to the convergence towards a period two cycle. This cycle can lose stability also (see figure Fig.17(b) where the system undergoes a period adding bifurcation after the period doubling one, with a short phase of chaos). Nevertheless, if we continue increasing the spike triggered parameter d , the cycle will collapse to a fixed point, via an inverted period-doubling bifurcation again.

The figure Fig.17 represents two cases for different v_r .

4.1.5 Bifurcations with respect to the input current

As already shown, the input current has a stabilizing effect on the dynamics. Here again, the same scheme appears, though less clearly since the dependency in I is quite different. Nevertheless the regularity of Φ with respect to I ensures us that the fixed point of Φ will become stable for I large enough via an inverted period doubling bifurcation. We simulated the orbits varying I in these cases and obtained the expected result for different values of the v_r parameter, large enough so that the map Φ is sharp. The results are presented in figure Fig.18

4.1.6 Cascade of period adding bifurcations and chaos with respect to v_r

A very interesting parameter would be the reset location v_r . As we will see in the simulations, the behavior of the system with respect to this parameter is very interesting and complex. The behavior of the set of curves Φ when varying v_r is not monotonous, and cannot be

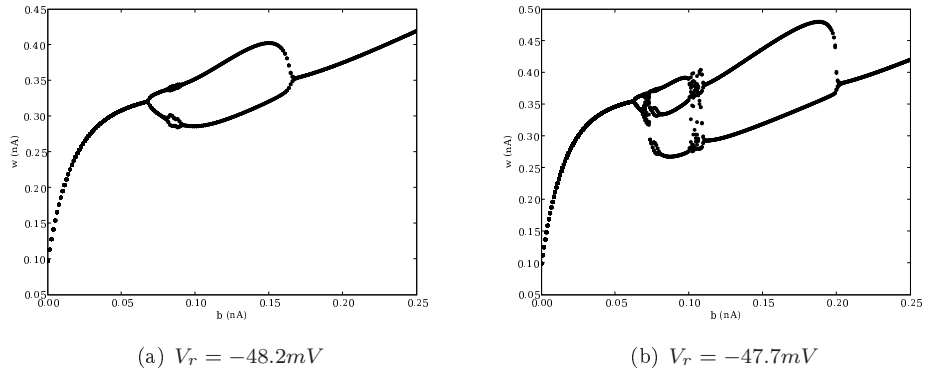


Figure 17: Orbits of Φ for different initial conditions, varying the spike-triggered adaptation parameter d , in the case of the dimensioned Adaptive Exponential model. We can observe that for d small enough the system converges towards the fixed point of Φ . When increasing d , as described in the text, the fixed point loses stability via a period doubling bifurcation and a cycle of period 2 appears. In the case (a) the system presents another period doubling bifurcation for $d \approx 0.8$, and then returns to equilibrium via an inverted period doubling bifurcation as described in the text. In the second simulation for V_r larger,

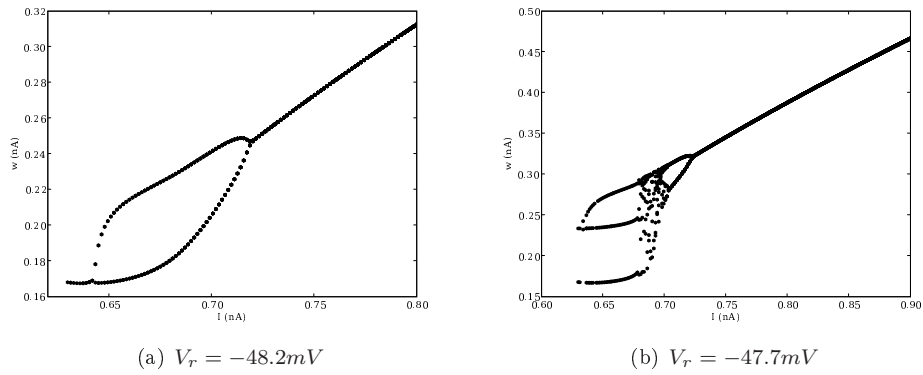


Figure 18: Orbits of Φ when varying the input current I in the case of the dimensioned Adaptive Exponential model. In the case 18(a) the reset location is small enough and the dynamics only presents a loss of stability via period doubling and then returns to equilibrium. In the second case 18(b), the fixed point is unstable when it appears and we have a period two cycle immediately followed by a period 3 cycle, then via an inverted period-adding bifurcation we return to a period two cycle, and then by inverted period doubling bifurcation to the fast-spiking equilibrium. The transition from period three to period two presents a chaotic behavior.

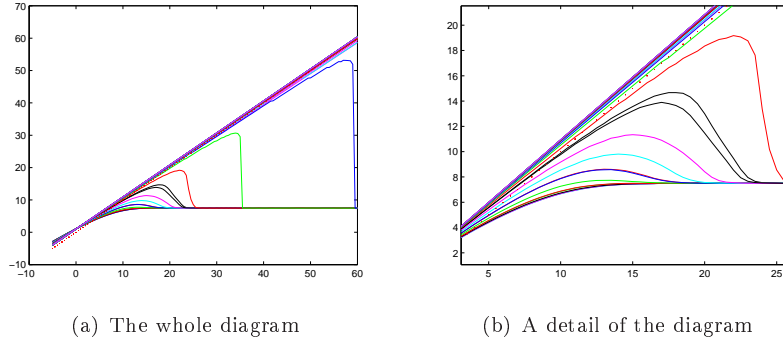
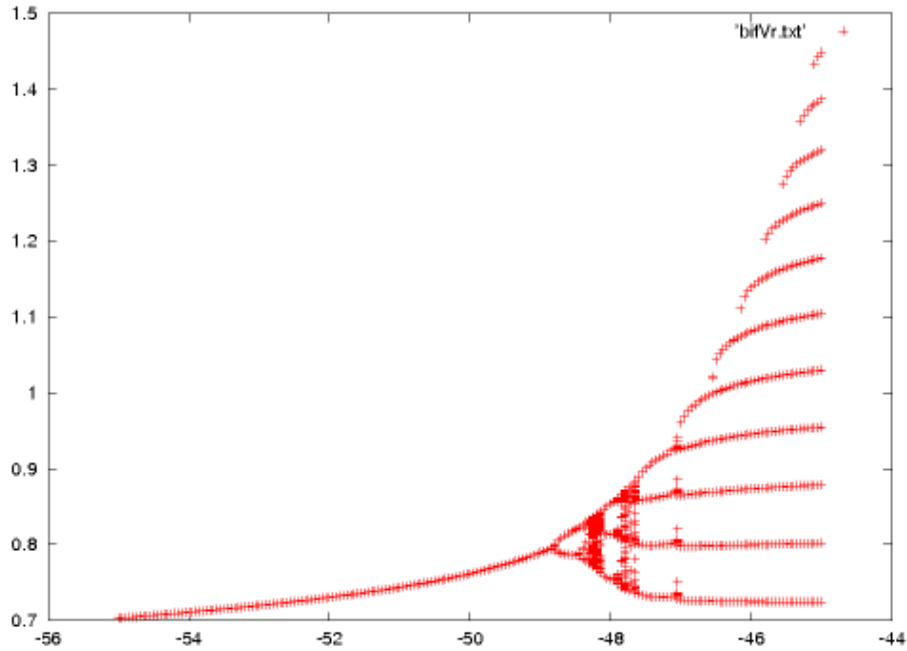


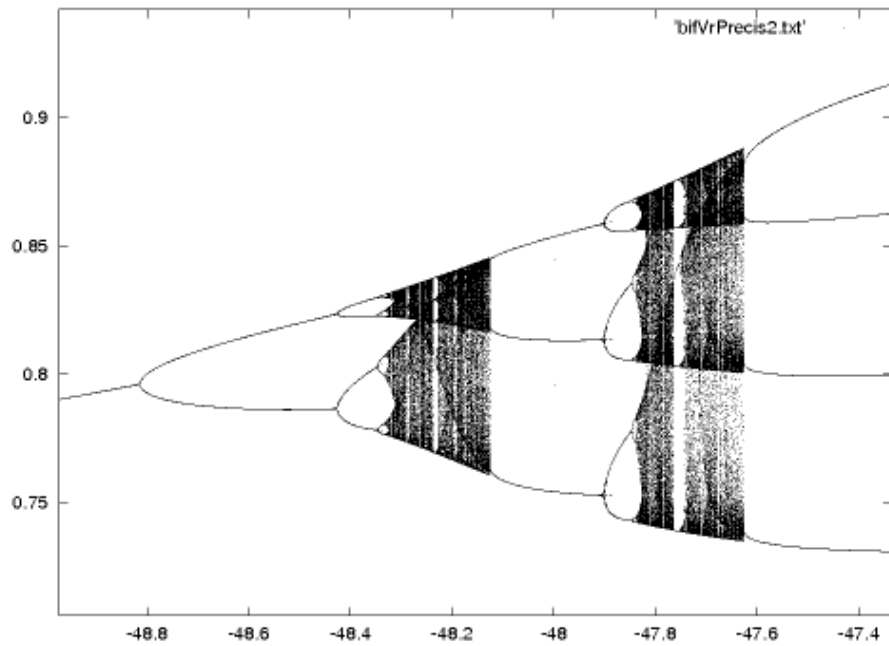
Figure 19: Poincaré application for the quartic model with $a = 1$, $b = 0.5$, $d = 1$, $I = 7$ and v_r ranging from -5 to 20 . The transition is very sharp, and the zoom let us see a little bit more precisely what happens before the fast change of Φ .

described very easily. First of all, the maximum of Φ , the point $w^* = F(v_r) + I$, will first decrease with v_r when v_r is inferior to the point where F takes its minimum, and then will increase again. The convexity of F makes the behavior of Φ quite sharp in function of v_r . Figure Fig.19 represents many curves when v_r varies. As we can see, for reasonable values of the parameter v_r , the curve Φ gets very sharp very fast and keeps sharper and sharper. As we see, the fixed point has a multiplier of absolute value strictly greater than 1 in the case presented for v_r large. It is also interesting to see that for very small values of v_r the Poincaré map is very flat.

If we study the fixed point and the stability of this map, we observe a very interesting behavior. The only fixed point loses quite fast its stability via a period doubling bifurcation. We numerically observe a cascade of period adding bifurcations. We also observed that the transition from period n to period $n + 1$ is done via a cascade of period doubling and a zone of chaos (see figure Fig.20). It is quite interesting to observe chaos in this model. Indeed, the firing patterns observed in the nervous system are often chaotic. For instance in the Purkinje cell, it has been observed that as the temperature increases for a given input current, the calcium spiking presented a period doubling during *in vitro* experiments (see [16, 5, 15, 8]). The appearance of doublets was also observed *in vivo* on recordings done by Jaeger and Bower on the ketamine-anesthetized guinea pig when the inhibition is blocked [12]. This type of route to chaos has also been shown in classical neuron models. For instance Rinzel and Miller in [18] located a period doubling on the interspike interval in the Hodgkin-Huxley model by computing eigenvalues along a family of periodic orbits. It has then been shown in other neuronal models, for instance in a version of the Hodgkin-Huxley model taking into account the temperature [6]. In this case, the system undergoes a period doubling cascade when varying the temperature.



(a) Full bifurcation diagram



(b) Zoom on the transitions

Figure 20: The period adding bifurcation cascade in the reset sequence for the adaptive integrate-and-fire neuron, for the original parameters (see [1]), with $a = 0.01$, and V_r ranging from $-55mV$ (original value), to $-43mV$, and a zoom on the transitions from fixed points to period 2, period 2 to period 3 and period 3 to period 4.

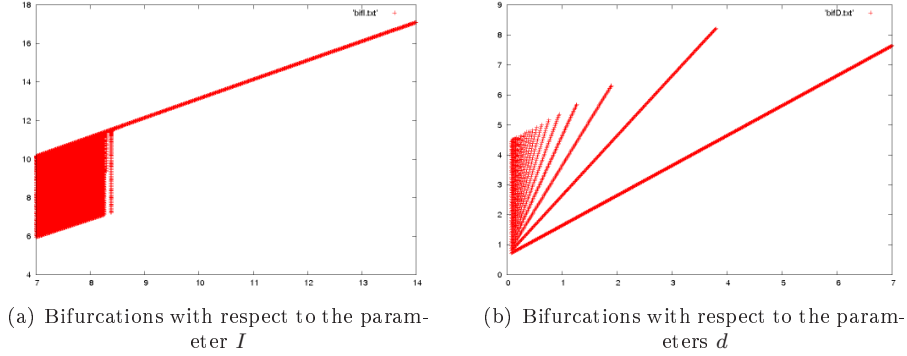


Figure 21: A RETIRER!!! Fixed points and fixed cycles in function of the adaptation parameter I and d . The period doubling observed generated strange behaviors which are stabilized when the parameters increase

In the figure Fig.20 we provide a diagram in the case of the adaptive exponential integrate-and-fire model. Indeed, this model has the advantage to be based on a biological analysis and has been fitted cautiously (see [1, 13]). For this reason we chose to instantiate the adaptive exponential neuron to be sure that the phenomenon occurs in a plausible range of values.

It is clear that this behavior influences the dependency in the other parameters, as we show in Figure fig.21.

4.2 Existence of a stable fixed point

In the case where $I < -\min(m(b), I^*(a, b))$ where $m(b)$ is the minimum of $G_b : x \mapsto F(x) - bx$ and $I^*(a, b) = bv_a - F(v_a)$ for v_a the unique solution of $F'(v_a) = a$, then there exists a stable fixed point and a saddle fixed point. The existence of the stable fixed point affects the shape of the definition domain \mathcal{D} .

First of all, let us study the cases when the attracting basin of the stable bounded trajectories (stable fixed points or stable limit cycles) is unbounded, for instance for the quadratic and quartic models.

In this case, as already stated, the dynamics will always be increasing on \mathcal{D} . The spiking behavior will depend on the relative position of $\Phi(w_{\max, \mathcal{D}})$ with respect to $w_{\max, \mathcal{D}}$:

1. If $\Phi(w_{\max, \mathcal{D}}) > w_{\max, \mathcal{D}}$ (i.e. $\Phi(\mathcal{D}) \not\subset \mathcal{D}$) then there will not exist any tonic behavior. Indeed, all a the spiking sequence will eventually exit from \mathcal{D} , because of the convexity property (see theorem 2.1). This will be the case for $v_r \in [v_-(I, b), v_+(I, b)]$.
2. If $\Phi(w_{\max, \mathcal{D}}) < w_{\max, \mathcal{D}}$ (i.e. $\Phi(\mathcal{D}) \subset \mathcal{D}$), then there will exist a stable fixed point and the spiking sequences will always converge to this fixed point (because the map Φ is

increasing and crosses the curve $y = x$, hence the derivative of Φ at this point will be positive and lower than 1) and any spiking sequence will be a regular spiking one. As in the case where there is no fixed point, the transient behavior that distinguishes between spike frequency adaptation and mixed mode will depend upon the multiplier of this fixed point).

This last case is the case of the bistability observed in the numerical experiments in [19, 10]. Hence for this type of models as the quadratic and quartic model, the bistability will always be regular spiking/rest. There will never be bursts or spiking variability (chaos) in these cases.

The case of the exponential adaptive model is quite different. Indeed, the attractor has not the same shape, and cycles can appear, which will correspond to a bistability bursting/rest.

1. If $v_r < v_{\min, \mathcal{D}}$ or $v_r > v_{\max, \mathcal{D}}$, then the above analysis when there is no fixed points remains valid.
2. If $v_r \in [v_{\min, \mathcal{D}}, v_{\max, \mathcal{D}}]$, then we distinguish two cases as before:
 - (a) if $\Phi(w_{\min, \mathcal{D}}) < w_{\min, \mathcal{D}}$ then we have $\Phi(\mathcal{D}) \subset \mathcal{D}$ and there exists a unique fixed point of Φ in I_1 which is stable because of the monotony and concavity properties of Φ on I_1 .
 - (b) if $\Phi(w_{\min, \mathcal{D}}) \in (w_{\min, \mathcal{D}}, w_{\max, \mathcal{D}})$ then the spiking dynamics will always be transient.
 - (c) if $\Phi(w_{\min, \mathcal{D}}) > w_{\max, \mathcal{D}}$, we can defined the sets where the neurons will spike at least n times for $n \in \mathbb{N}$:

$$\mathcal{D}_n = \mathcal{D} \setminus \Phi^{-1}(\mathcal{D}) \setminus \dots \setminus (\Phi^{-1})^{n-1}(\mathcal{D})$$

and the definition definition domain of the tonic behavior is defined by:

$$\mathcal{D}_\infty = \mathcal{D} \setminus \Phi^{-1}((w_{\min, \mathcal{D}}, w_{\max, \mathcal{D}}) \setminus \dots \setminus (\Phi^{-1})^n((w_{\min, \mathcal{D}}, w_{\max, \mathcal{D}})) \dots$$

(see Fig.22). This structure is quite similar to the definition domain of the logistic map for $\mu > 4$ (see [3]). This case does not occur a biological range of parameters, since the extension of the attraction basin of the stable fixed point is quite wide. Nevertheless, it is interesting to note that in this case, there exists lots of particular behaviors

4.3 Existence of a stable limit cycle

If the nonlinearity satisfies the property $F'''(v_a) < 0$ where v_a is the unique solution of $F'(v_a) = a$, then there exists a stable limit cycle for $b > a - \frac{F''(v_a)^2}{F'''(v_a)}$ and $I^*(a, b) < I < -m(b)$.

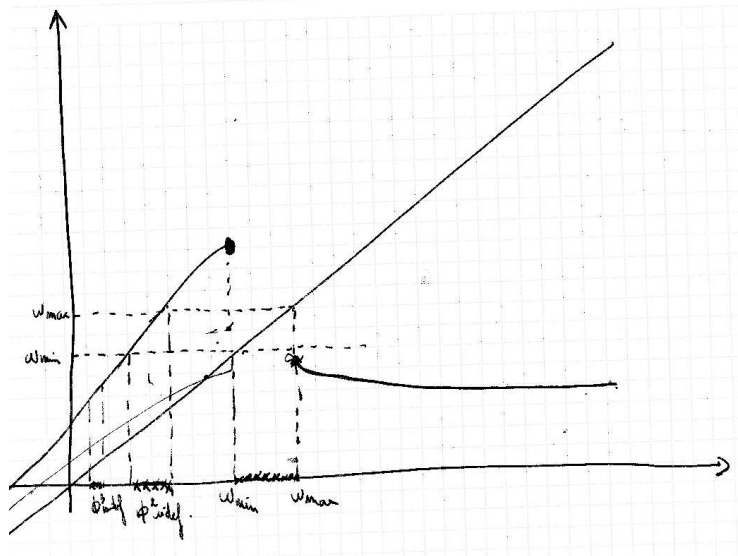
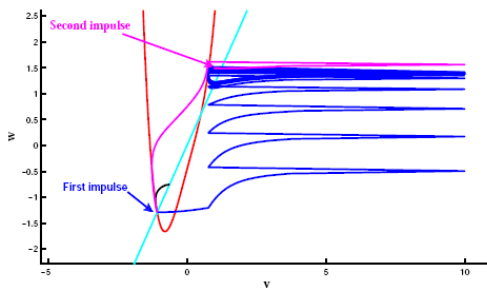
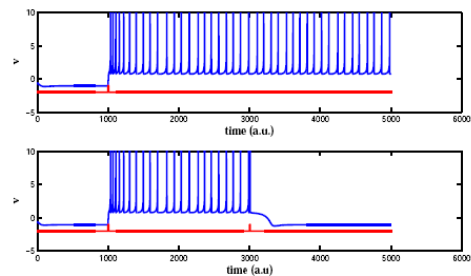


Figure 22: Definition set of the tonic spiking in the case 2c



(a) Bistability: return to equilibrium via the same impulse



(b) Bistability

Figure 23: Bistability in the case of the quartic model

This is the case for instance for the quartic model. As shown numerically (See Fig.2(a)), the attraction basin of the limit cycle for the quartic model is unbounded. Hence in \mathcal{D} , the map Φ is increasing, and we have:

- if $\Phi(w_{\max, \mathcal{D}}) > w_{\max, \mathcal{D}}$ (for instance in the case where $v_-(I, b) < v_r < v_+(I, b)$), then every trajectory will fall in the attraction basin of the cycle after a finite number of spikes emitted.
- if $\Phi(w_{\max, \mathcal{D}}) \leq w_{\max, \mathcal{D}}$ then \mathcal{D} will be stable under Φ (i.e. $\Phi(\mathcal{D}) \subset \mathcal{D}$ and there exists a stable fixed point for Φ in \mathcal{D}). Any sequence of iterates starting from \mathcal{D} will converge to this fixed point. Hence there will a bistable behavior: a stable regular spiking behavior and a stable subthreshold oscillation.

4.4 No stable bounded trajectory

In this section we consider the case where there is no stable fixed point nor stable limit cycle. This case corresponds in the cases where $F'''(v_a) > 0$ (resp. $F'''(v_a) < 0$) to the case where $b > a$ (resp $a < b < a - \frac{F''(v_a)}{F'''(v_a)}$) and $I^*(a, b) < I < -m(b)$ where $I^*(a, b) = bv_a - F(v_a)$ for v_a the unique solution of $F'(v_a) = a$, and $m(b)$ the unique minimum of the function $G_b(x) = F(x) - bx$ (see [19]). In this case, the system has two unstable fixed points (a saddle fixed point and a repulsive one).

- If $v_r < V_{\min}$, then the analysis done in the case where there is no fixed point applies directly. Nevertheless in that case, v_r is bounded and hence it is not possible to sharpen the map Φ as we did in the section of the chaos by taking v_r large enough, and hence bursts and chaos are less probables in that case.
- If there is no fixed point for the map Φ (for instance if the identity line crosses the discontinuity), then regular spiking is impossible, and hence we will have bursts or irregular spiking necessarily.
- If there is a unique fixed point, then regular spiking and bursts can coexist depending on the initial condition. Indeed, the map Φ is discontinuous and can present stable cycles together with the presence of a stable fixed point. For instance assume that $v_r < v_+$. In this case, denote by w_d is the discontinuity point (the intersection of $v = v_r$ with the stable manifold of the saddle fixed point). We have $w_d < w^*$. If furthermore $\Phi(w_d^-) < w_d$, then the image of (w_d, ∞) by Φ is included in $(-\infty, w_d)$ which is stable under the action of Φ . Hence the dynamics of Φ is after possible one iteration described by the dynamics of Φ on $(-\infty, w_d)$. It is easy to prove that in this case the sequence converges towards the fixed point of Φ . This proof readily extends to the case where $v_r > v_+$ and $\max_{x \in (-\infty, w_d)} < w_d$.
- The case where there are many fixed points is way more complex. In this case the system could have different regular spiking frequencies, depending on the initial condition.

In this case of multiple attractors, the system could switch between these attractors, present hysteresis, and its computational capabilities are increased.

References

- [1] R. Brette and W. Gerstner. Adaptive exponential integrate-and-fire model as an effective description of neuronal activity. *Journal of Neurophysiology*, 94:3637–3642, 2005.
- [2] Romain Brette. The cauchy problem for one-dimensional spiking neuron models. *Cognitive Neurodynamics*, 2(1):21–27, 2007.
- [3] R.L. Devaney. *An Introduction to Chaotic Dynamical Systems*. Westview Press, 2003.
- [4] Jean Dieudonné. *Éléments d’analyse - Tome I : Fondements de l’analyse moderne*. Gauthier-Villars, 1963.
- [5] Y. Etzion and Y. Grossman. Potassium currents modulation of calcium spike firing in dendrites of cerebellar Purkinje cells. *Experimental Brain Research*, 122(3):283–294, 1998.
- [6] U. Feudel, A. Neiman, X. Pei, W. Wojtenek, H. Braun, M. Huber, and F. Moss. Homoclinic bifurcation in a Hodgkin–Huxley model of thermally sensitive neurons. *Chaos: An Interdisciplinary Journal of Nonlinear Science*, 10:231, 2000.
- [7] N. Fourcaud-Trocme, D. Hansel, C. van Vreeswijk, and N. Brunel. How Spike Generation Mechanisms Determine the Neuronal Response to Fluctuating Inputs. *Journal of Neuroscience*, 23(37):11628, 2003.
- [8] J. Hounsgaard and J. Midtgaard. Synaptic control of excitability in turtle cerebellar Purkinje cells. *The Journal of Physiology*, 409:157, 1989.
- [9] E. Izhikevich. Simple model of spiking neurons. *IEEE Transactions on Neural Networks*, 14(6):1569–1572, 2003.
- [10] E.M. Izhikevich. Which model to use for cortical spiking neurons? *IEEE Trans Neural Netw*, 15(5):1063–1070, September 2004.
- [11] Eugene M. Izhikevich. *Dynamical Systems in Neuroscience: The Geometry of Excitability and Bursting*. The MIT Press, 2006. To appear.
- [12] D. Jaeger and J.M. Bower. Prolonged responses in rat cerebellar Purkinje cells following activation of the granule cell layer: an intracellular in vitro and in vivo investigation. *Experimental Brain Research*, 100(2):200–214, 1994.
- [13] R. Jolivet, R. Kobayashi, A. Rauch, R. Naud, S. Shinomoto, and W. Gerstner. A benchmark test for a quantitative assessment of simple neuron models. *Journal of Neuroscience Methods*, 169(2):417–424, 2008.
- [14] T.Y. Li and J. Yorke. Period three implies chaos. *American Mathematical Monthly*, 82:985–992, 1975.
- [15] R. Llinas and M. Sugimori. Electrophysiological properties of in vitro Purkinje cell somata in mammalian cerebellar slices. *The Journal of Physiology*, 305(1):171–195, 1980.
- [16] Y. Mandelblat, Y. Etzion, Y. Grossman, and D. Golomb. Period Doubling of Calcium Spike Firing in a Model of a Purkinje Cell Dendrite. *Journal of Computational Neuroscience*, 11(1):43–62, 2001.
- [17] R Naud, N Macille, C Clopath, and W Gerstner. Firing patterns in the adaptive exponential integrate-and-fire model. *Biological Cybernetics (submitted)*, 2008.
- [18] J. Rinzel and R.N. Miller. Numerical calculation of stable and unstable periodic solutions to the Hodgkin–Huxley equations. *Math. Biosci*, 49:27–59, 1980.
- [19] Jonathan Touboul. Bifurcation analysis of a general class of nonlinear integrate-and-fire neurons. *SIAM Journal on Applied Mathematics*, 68(4):1045–1079, 2008.
- [20] Jonathan Touboul and Romain Brette. Dynamics and bifurcations of the adaptive exponential integrate-and-fire model. *Biological Cybernetics (submitted)*, 2008.



Unité de recherche INRIA Sophia Antipolis
2004, route des Lucioles - BP 93 - 06902 Sophia Antipolis Cedex (France)

Unité de recherche INRIA Futurs : Parc Club Orsay Université - ZAC des Vignes
4, rue Jacques Monod - 91893 ORSAY Cedex (France)

Unité de recherche INRIA Lorraine : LORIA, Technopôle de Nancy-Brabois - Campus scientifique
615, rue du Jardin Botanique - BP 101 - 54602 Villers-lès-Nancy Cedex (France)

Unité de recherche INRIA Rennes : IRISA, Campus universitaire de Beaulieu - 35042 Rennes Cedex (France)

Unité de recherche INRIA Rhône-Alpes : 655, avenue de l'Europe - 38334 Montbonnot Saint-Ismier (France)

Unité de recherche INRIA Rocquencourt : Domaine de Voluceau - Rocquencourt - BP 105 - 78153 Le Chesnay Cedex (France)

Éditeur
INRIA - Domaine de Voluceau - Rocquencourt, BP 105 - 78153 Le Chesnay Cedex (France)
<http://www.inria.fr>
ISSN 0249-6399